



**HAL**  
open science

## **Hydrological response of Andean catchments to recent glacier mass loss**

Alexis Caro, Thomas Condom, Antoine Rabatel, Nicolas Champollion, Nicolás García, Freddy Saavedra

### ► **To cite this version:**

Alexis Caro, Thomas Condom, Antoine Rabatel, Nicolas Champollion, Nicolás García, et al.. Hydrological response of Andean catchments to recent glacier mass loss. *The Cryosphere*, 2024, 18 (5), pp.2487-2507. <10.5194/tc-18-2487-2024>. <hal-04792468>

**HAL Id: hal-04792468**

**<https://hal.science/hal-04792468v1>**

Submitted on 22 Nov 2024

**HAL** is a multi-disciplinary open access archive for the deposit and dissemination of scientific research documents, whether they are published or not. The documents may come from teaching and research institutions in France or abroad, or from public or private research centers.

L'archive ouverte pluridisciplinaire **HAL**, est destinée au dépôt et à la diffusion de documents scientifiques de niveau recherche, publiés ou non, émanant des établissements d'enseignement et de recherche français ou étrangers, des laboratoires publics ou privés.



Distributed under a Creative Commons CC BY 4.0 - Attribution - International License



# Hydrological response of Andean catchments to recent glacier mass loss

Alexis Caro<sup>1</sup>, Thomas Condom<sup>1</sup>, Antoine Rabatel<sup>1</sup>, Nicolas Champollion<sup>1</sup>, Nicolás García<sup>2</sup>, and Freddy Saavedra<sup>3</sup>

<sup>1</sup>Univ. Grenoble Alpes, CNRS, IRD, INRAE, Grenoble-INP, Institut des Géosciences de l'Environnement (IGE, UMR 5001), 38000 Grenoble, France

<sup>2</sup>Glaciología y Cambio Climático, Centro de Estudios Científicos (CECs), Valdivia, Chile

<sup>3</sup>Departamento de Ciencias Geográficas, Facultad de Ciencias Naturales y Exactas, Universidad de Playa Ancha, Leopoldo Carvallo 270, Playa Ancha, Valparaíso, Chile

**Correspondence:** Alexis Caro (alexis.caro.paredes@gmail.com)

Received: 3 May 2023 – Discussion started: 23 May 2023

Revised: 14 March 2024 – Accepted: 2 April 2024 – Published: 22 May 2024

**Abstract.** The impacts of the accelerated glacier retreat in recent decades on glacier runoff changes are still unknown in most Andean catchments, increasing uncertainties in estimating water availability. This particularly affects the outer tropics and Dry Andes, heavily impacted by prolonged droughts. Current global estimates overlook climatic and morphometric disparities, which significantly influence model parameters, among Andean glaciers. Meanwhile, local studies have used different approaches to estimate glacier runoff in a few catchments. Improving 21st-century glacier runoff projections relies on calibrating and validating models using corrected historical climate inputs and calibrated parameters across diverse glaciological zones. Here, we simulate glacier evolution and related runoff changes between the periods 2000–2009 and 2010–2019 across 786 Andean catchments (11 282 km<sup>2</sup> of glacierized area, 11° N to 55° S) using the Open Global Glacier Model (OGGM). TerraClimate atmospheric variables were corrected using in situ data, getting a mean temperature bias by up to 2.1 °C and enhanced monthly precipitation. Glacier mass balance and volume were calibrated, where melt factor and the Glen A parameter exhibited significant alignment with varying environmental conditions. Simulation outcomes were validated against in situ data in three documented catchments (with a glacierized area > 8 %) and monitored glaciers. Our results at the Andes scale reveal an average reduction of 8.3 % in glacier volume and a decrease of 2.2 % in surface area between the periods 2000–2009 and 2010–2019. Comparing these two periods, glacier and climate variations have led to a 12 % increase in mean

annual glacier melt (86.5 m<sup>3</sup> s<sup>-1</sup>) and a decrease in rainfall on glaciers of –2 % (–7.6 m<sup>3</sup> s<sup>-1</sup>) across the Andes, with both variables comprising the glacier runoff. We confirmed the utility of our corrected regional simulations of glacier runoff contribution at the catchment scale, where our estimations align with previous studies (e.g., Maipo 34° S, Chile) as well as provide new insights on the seasonal glaciers' largest contribution (e.g., La Paz 16° S, Bolivia) and new estimates of glacier runoff contribution (e.g., Baker 47° S, Chile).

## 1 Introduction

The largest glacierized area in the Southern Hemisphere outside the Antarctic ice sheet is found in the Andes (RGI Consortium, 2017; Masiokas et al., 2020). Andean glaciers supply water for roughly 45 % of the population in the Andean countries (Devenish and Gianella, 2012) and for ecosystems (Zimmer et al., 2018; Cauvy-Fraunié and Dangles, 2019). Continuous glacier shrinkage has been detected since the late 1970s, with intensification observed over the past two decades (Rabatel et al., 2013; Dussailant et al., 2019; Masiokas et al., 2020). Glacier volume loss has helped modulate river discharges, mainly in dry seasons (e.g., Baraer et al., 2012; Soruco et al., 2015; Guido et al., 2016; Ayala et al., 2020).

Few studies have estimated glacier changes and their effects on hydrology using observation or modeling focused on specific Andean catchments. For instance, the global-scale

study by Huss and Hock (2018) comprised 12 Andean catchments (1980–2100). They defined glacier runoff as all the meltwater and rainfall coming from the initially glacierized area, as given by the Randolph Glacier Inventory version 4.0, and found an increase in glacier runoff in the tropical and Dry Andes until 2020, but a more contrasted signal in the Wet Andes: no glacier runoff change was observed in some catchments, whereas others showed a reduction or an increase. However, their estimations overlook the diversity in climate conditions and glacier morpho-topography, such as latitudinal and/or longitudinal climate variations and glacier characteristics (glacier size, slope, and aspect), across the Andes and inside large catchments (Caro et al., 2021). This affects the simulation results, as they heavily rely on climate inputs and calibrated parameters. For instance, varying temperature lapse rates could result in significant disparities in glacier melt and the determination of solid and liquid precipitation on glaciers (Schuster et al., 2023). Furthermore, the selection of precipitation factor values is also crucial. Based on local studies, the glacier runoff contribution (glacier runoff relative to the total catchment runoff) in the tropical Andes was estimated to be around 12 % and 15 % in the Río Santa (9° S) and La Paz (16° S) catchments, respectively (Mark and Seltzer, 2003; Soruco et al., 2015). For the La Paz catchment, Soruco et al. (2015) found no change in the glacier runoff contribution for the period 1997–2006 compared with the longer 1963–2006 period. This was attributed to the fact that the glacier surface reduction over the time period was compensated by their increasingly negative mass balance. In the Dry Andes, the Huasco (29° S), Aconcagua (33° S), and Maipo (34° S) catchments showed a glacier runoff contribution comprising between 3 % and 23 % for different catchment sizes between 241 and 4843 km<sup>2</sup> (Gascoïn et al., 2011; Ragetti and Pellicciotti, 2012; Ayala et al., 2020). These catchments had mainly negative glacier mass balances which were slightly interrupted during El Niño episodes (2000–2008), thereby reducing glacier runoff. In the Wet Andes, Dussaillant et al. (2012) estimated that some catchments in the Northern Patagonian Icefield are strongly conditioned by glacier melting. In addition, Huss and Hock (2018) did not identify changes in the glacier runoff of the Baker catchment between 1980 and 2000. However, these studies focused on a restricted number of catchments, employing diverse input data and methodologies over different periods. As such, these local estimations may not be indicative of the broader trends across the entire Andean region. Notably, even neighboring glacierized catchments can exhibit substantial variations in climatic and topographic characteristics (Caro et al., 2021).

Nowadays, the availability of global glaciological products, such as glacier surface elevation differences and glacier volume estimation (Farinotti et al., 2019; Hugonnet et al., 2021; Millan et al., 2022), allows for large-scale glacio-hydrological simulations with the possibility of accurately calibrating and validating numerical models at the glacier scale. In addition, modeling frameworks, such as the Open

Global Glacier Model (OGGM, Maussion et al., 2019), have been implemented to simulate the glacier mass balance and glacier dynamics at a global scale. Therefore, OGGM and the glaciological global dataset, in combination with in situ meteorological and glaciological measurements, considering the differences in Andean glaciological zones, can be used to quantify the glacier retreat and the related hydrological responses at the catchment scale across the Andes while taking the related uncertainties into account. Currently, reconstructions of glacier surface mass balance across the Andes (9–52° S) rely on a temperature-index model. Notably, higher mean melt factor values are identified in the tropical Andes (0.3–0.5 mm h<sup>-1</sup> °C<sup>-1</sup>), compared with the Dry Andes (0.3–0.4 mm h<sup>-1</sup> °C<sup>-1</sup>) and Wet Andes (0.1–0.5 mm h<sup>-1</sup> °C<sup>-1</sup>) (e.g., Fukami and Naruse, 1987; Koizumi and Naruse, 1992; Stuefer, 1999; Takeuchi et al., 1995; Rivera, 2004; Sicart et al., 2008; Condom et al., 2011; Caro, 2014; Huss and Hock, 2015; Bravo et al., 2017).

Here, using OGGM, we estimate the glacier changes (area and volume) and the consecutive hydrological responses called glacier runoff (which is composed of glacier melt, as the addition of ice melt and snowmelt, as well as rainfall on glaciers) for 786 catchments across the Andes (11° N to 55° S) with a glacierized surface of at least 0.01 % for the period 2000–2019. This approach allows us to study the behavior of glaciers across the entire Andes and within specific catchments (for instance, those previously studied). Considering the significant hydro-glaciological variations in neighboring catchments and the potential biases within climatic datasets, the air temperature and precipitation data from the TerraClimate dataset (Abatzoglou et al., 2018) were corrected using in situ data across the Andes. On the other hand, the simulation procedure considered the calibration of glacier surface mass balance and glacier volume. Both, corrections of climate as well as calibrations (at the glacier scale), were performed considering the climatic and morphometric differences in the Andes, represented through the glaciological zones (Caro et al., 2021). Given that the most important uncertainties in simulating future glacier evolution come from, among other factors, the implementation of the models during the historical period, we validate our simulation and calibration outcomes against observed data from glaciers and catchments.

Section 2 presents the data and methods. In Sect. 3, we describe the glacier changes and hydrological responses at the glaciological zone and catchment scales across the Andes. In Sect. 4, we discuss our results and the main steps forward compared with previous research.

## 2 Data and methods

This section comprises the processed data used as input and during the modeling framework (Fig. 1).

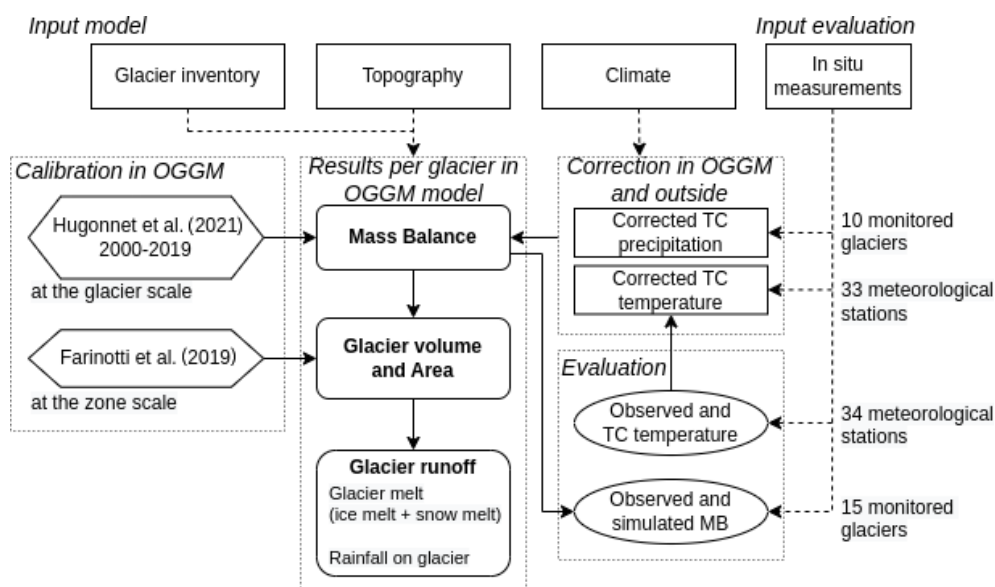


**Figure 1.** Workflow per simulated glacier using OGGM between 2000 and 2019. Two groups of input data were used: one to run OGGM and the second to correct/evaluate the TerraClimate temperature ( $cTC_t$ ) and precipitation ( $cTC_p$ ). Then, the mass balance and glacier volume were calibrated. Lastly, results such as the  $cTC_t$  and glacier mass balance were evaluated at 34 meteorological stations and on 15 glaciers with mass balance observations. The corrections in OGGM and outside box refer to analyses performed by running the model and also analyzing data outside the model tool. An example is the estimation of temperature lapse rates, which were estimated from in situ measurements but introduced in the OGGM model as a parameter value.

## 2.1 Data collection and preprocessing

### 2.1.1 Historical climate data

We used two climate datasets: the TerraClimate reanalysis (“Climate” box in Fig. 1) and in situ measurements from meteorological stations (“In situ measurements” box in Fig. 1). TerraClimate is based on reanalysis data since 1958, with a 4 km grid size at a monthly timescale, and was validated with the Global Historical Climatology Network (temperature:  $r = 0.95$  and mean absolute error (MAE) =  $0.32\text{ }^\circ\text{C}$ ; precipitation:  $r = 0.9$  and MAE =  $9.1\%$ ) (Abatzoglou et al., 2018). The mean temperature was estimated from the maximum and minimum temperatures, whereas precipitation data are accumulated on a monthly basis. The meteorological records were compiled from Andean organizations and scientific reports (Rabatel et al., 2011; MacDonell et al., 2013; Schaefer et al., 2017; CECs, 2018; Shaw et al., 2020; Hernández et al., 2021; CEAZA, 2022; DGA, 2022; GLACIOCLIM, 2022; IANIGLA, 2022; Mateo et al., 2022; SENAMHI, 2022). The mean monthly air temperature measurements were taken from 35 off-glacier and on-glacier meteorological stations, the latter being rare, located between  $9$  and  $51^\circ\text{S}$ . However, it is important to note that long-term measurements were not available northward of  $9^\circ\text{S}$  (the inner tropics, IT). To address this, data from stations located in the outer tropics (OT) were used as a reference for temperature corrections in this zone, which could affect the performance in the estimation of cal-

ibrated parameters such as the melt factor. The location and main properties of the meteorological stations are shown in Table S1 in the Supplement.

### 2.1.2 Climatic data correction and evaluation

For the temperature variable, we first quantified the local vertical annual temperature lapse rates using the in situ measurements for 33 sites across the Andes (see Table S1 and Fig. S1 in the Supplement). Then, the TerraClimate temperature was corrected with these in situ records so that they could be used in the simulations (“Correction” box in Fig. 1). Lastly, the corrected TerraClimate temperature was evaluated via a comparison with the 34 in situ data (“Evaluation” box in Fig. 1). Conversely, the precipitation variable from the TerraClimate reanalysis was scaled using the mass balance measurements for 10 monitored glaciers and was evaluated for 15 glaciers (“Correction” and “Evaluation” boxes in Fig. 1). Specific data are available in Tables S3–S5.

Vertical temperature lapse rates (LRs) from the in situ records were estimated for each glaciological zone across the Andes as per Gao et al. (2012). The temperature LRs are presented in Fig. S1. These gradients were applied to correct the raw TerraClimate temperature on the glaciers ( $rTC_t$ ). The corrected TerraClimate temperature at the mean elevation of glacier ( $cTC_t$ ) was calculated using the following equation:

$$cTC_t = rTC_t + \Gamma \cdot \Delta h, \quad (1)$$

where  $\Gamma$  is the temperature LR estimated here and  $\Delta h$  is the elevation difference between a glacier elevation and the mean elevation of the TerraClimate grid cell where the glacier is located.

Then, we assessed the  $cTC_t$  in meteorological station locations (9–51° S) on a monthly scale, paying attention to the monthly variability in temperature as well as to the mean temperature for all the periods with data. The  $cTC_t$  monthly mean variability was evaluated using the Pearson correlation coefficient, whereas the mean temperature for the whole period considered the mean difference between  $cTC_t$  and the observed temperature (biases).

In addition, the total precipitation was scaled ( $cTC_p$ ) using precipitation factors ( $P_f$ ) for each glaciological zone across the Andes. (See the relationship between solid precipitation and  $P_f$  in Eq. 3.) In a second step we discriminated between snowfall and rainfall using a linear regression between the temperature thresholds to obtain the solid and liquid precipitation fraction (Maussion et al., 2019). We ran 31 simulations for 18 glaciers with mass balance measurements across the Andes using  $P_f$  values between 1 and 4 taking previous studies into account (Masiokas et al., 2016; Burger et al., 2019; Fariás-Barahona et al., 2020). Ultimately, 10 glaciers were selected (see Table S3), because their simulated mass balances showed a closer standard deviation in comparison with measurements. The goal was to find the closest simulated mass balance standard deviation ( $simSD_{mb}$ ) in comparison with the measured mass balance standard deviation ( $obsSD_{mb}$ ) using different  $P_f$  values (Eq. 2):

$$P_f = \{1 \leq P_f \leq 4 : simSD_{mb} \approx obsSD_{mb}\}. \quad (2)$$

A similar methodology was proposed by Marzeion et al. (2012) and Maussion et al. (2019). The results of the closest simulated mass balance standard deviations and associated  $P_f$  are presented in Table S3. The simulated annual mass balance was evaluated on 15 monitored glaciers using a Pearson correlation coefficient and bias (as the average difference) from simulated mass balance and measured mass balance (“Evaluation” box in Fig. 1). In addition, details such as snow/rainfall partitioning are described hereafter and in the model implementation (Sect. 2.2).

### 2.1.3 Glacier data

#### Glacier inventory

We used version 6.0 of the Randolph Glacier Inventory (RGI Consortium, 2017) to extract the characteristics of each glacier, e.g., location, area, and glacier front in land or water (“Glacier inventory” box in Fig. 1). The RGI v6.0 was checked using the national glacier inventories compiled by Caro et al. (2021), filtering every RGI glacier that was not found in the national glacier inventories, to obtain a total glacierized surface area of 30 943 km<sup>2</sup> (filtering 633 km<sup>2</sup>). The glacier extent in the RGI v6.0 is representative of that

of the early 2000s. The analysis by catchment and glaciological zones is related to the locations and elevation of these glaciers. Overall, 36 % of the total glacierized surface area across the Andes is considered. Over 85 % of the glacierized surface area in the Dry Andes (18–37° S) and 79 % in the tropical Andes (11° N to 18° S) are considered, which corresponds to 11 % (3377 km<sup>2</sup>, in 321 catchments) of the total glacierized area of the Andes. For the Wet Andes (37–55° S), 29 % of the glacierized surface area in the region is considered, which corresponds to 26 % (7905 km<sup>2</sup>, in 465 catchments) of the total glacierized area in the Andes. (See the distribution of the catchments in Fig. 2a.) The simulated glacierized surface area is lower in the Wet Andes due to the filtering out of the numerous calving glaciers found there.

#### Glacier mass balance

The mass balance datasets were composed of the global glacier surface elevation change product of Hugonnet et al. (2021) (“Calibration” box in Fig. 1) and in situ measurements of the glacier surface mass balance (“Evaluation” box in Fig. 1) since 2000 from different institutions (e.g., Marangunic et al., 2021; WGMS, 2021). The Hugonnet et al. (2021) product was quantified for each glacier using the OGGM toolbox (Fig. 2d). Then, the geodetic mass balance estimates were obtained for every glacier of the RGI v6.0. In situ measurements of the glacier surface mass balance are available between 5° N and 55° S (across all Andean regions) at the hydrological year scale (dates vary according to the latitude). However, the tropical Andes region is represented by just two glaciers (Conejeras and Zongo glaciers), producing an underrepresentation in the evaluation of the simulated mass balance in this region. The location and main characteristics of the 18 monitored glaciers are shown in Table S4.

#### Glacier volume

The global glacier ice thickness product of Farinotti et al. (2019) was used to calibrate each glacier of the RGI v6.0 in OGGM (“Calibration” box in Fig. 1). Farinotti et al. (2019) pooled the outputs of five different models to determine the distribution of the ice thickness on 215 000 glaciers outside the Greenland and Antarctic ice sheets.

### 2.1.4 Glaciological zones and catchments

A total of 11 glaciological zones across the Andes were compiled from Caro et al. (2021) and all glaciers northward of the outer tropics were considered as zone number 12, called the inner tropics. To identify the glacierized area in each catchment, a spatial intersection was made between the glaciers identified in the filtered RGI v6.0 and the level-9 HydroSHEDS catchments (Lehner and Grill, 2013). Then, we considered catchments with a glacierized surface area  $\geq 0.01$  % (max = 62 %, mean = 5 %, and median = 2 %). We selected 786 catchments with a surface

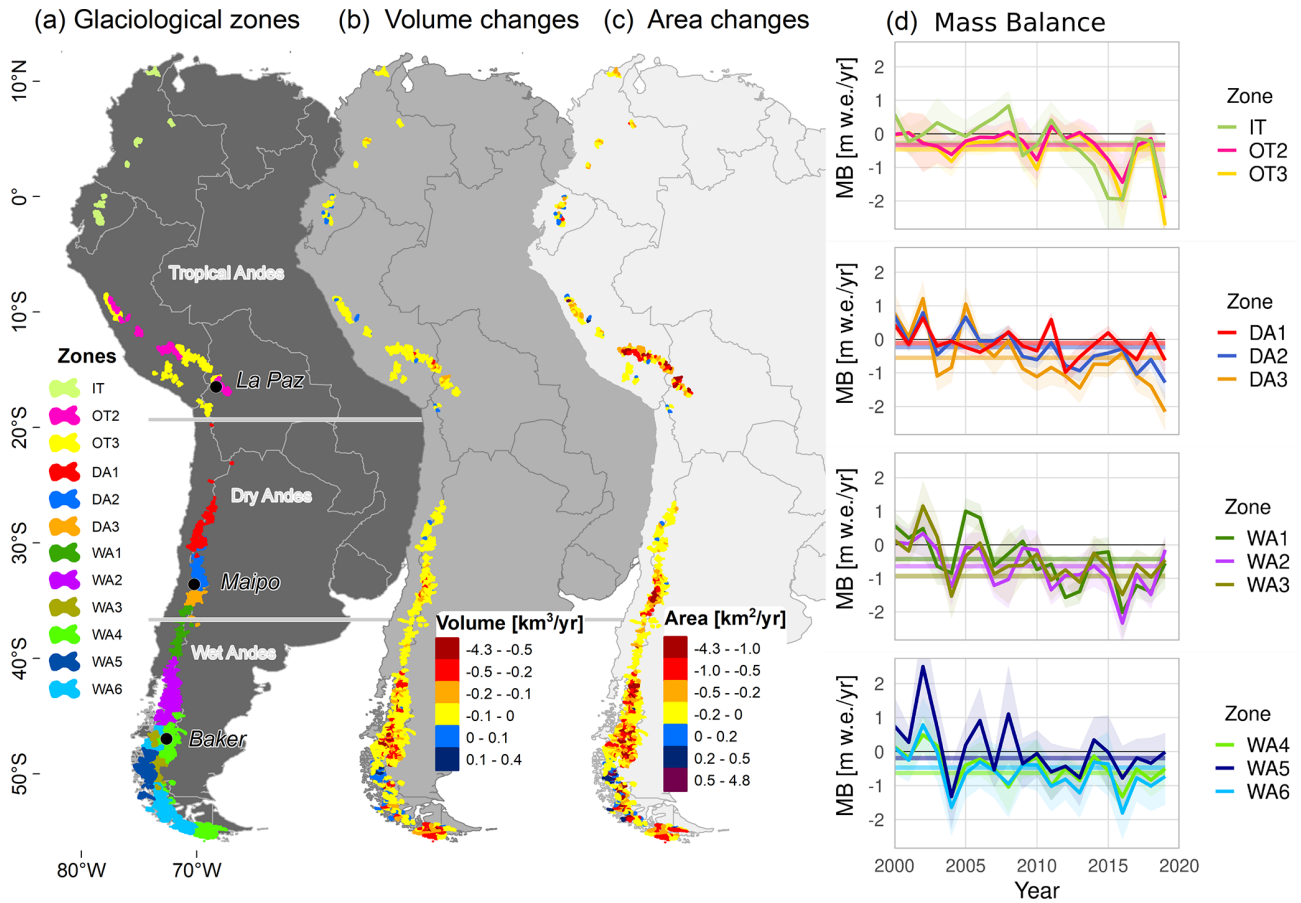


**Figure 2.** Recent glacier changes across the Andes. The glacier changes represent the mean annual differences between the periods 2000–2009 and 2010–2019 per catchment ( $n = 786$ ). Panel (a) shows the distribution of the glaciological zones (11° N to 55° S), followed by the (b) volume and (c) area changes at the catchment scale. The (d) annual specific mass balances are presented in each glaciological zone (the shaded areas are the standard deviation), where the straight lines correspond to the mean geodetic mass balance (2000–2019) estimated by Hugonnet et al. (2021).

area between 3236 and 20 km<sup>2</sup> across the Andes (11° N to 55° S), including 13 179 glaciers with a total surface area of 11 282 km<sup>2</sup> (36 % of the total glacierized surface area in the Andes).

Calving glaciers (lake- and marine terminating; 15 444 km<sup>2</sup>), primarily located in the Northern and Southern Patagonian Icefields as well as in the Cordillera Darwin, were not considered because the calving process implemented in this version of OGGM (1.5.3) which relies on Hugonnet et al. (2021) data to calibrate the simulated mass balance could exhibit significant uncertainty when applied to these particular glaciers. In this regard, Zhang et al. (2023) estimated an underestimation of glacier mass loss for lake-terminating glaciers using geodetic methods, accounting for a subaqueous mass loss of 10 % ± 4 % in the central Himalaya during the period 2000–2020. Their findings revealed that the total mass loss for certain glaciers was underestimated by as much as 65 % ± 43 %. The glaciers that were not simulated for the internal model inconsistencies

account for less than 1 % of the total glacierized surface area. The other remaining 4514 km<sup>2</sup> filtered glacierized surface area corresponds to glacierized catchments that present an increase in glacier volume but a reduction in the glacierized surface area. Only 59 km<sup>2</sup> was associated with glaciers filtered in the outer tropics 1 zone.

We selected the La Paz (Sorucu et al., 2015), Maipo (Ayala et al., 2020), and Baker (Dussaillant et al., 2012) catchments located in glaciological regions with different climatic and morphometric characteristics (Caro et al., 2021) to evaluate our simulations in terms of glacier changes and glacier runoff contributions over the period 2000–2019. In the La Paz and Maipo catchments, previous hydro-glaciological studies have quantified the impact of glacier changes and their hydrological contribution. However, these studies often overlook relevant processes such as variations in precipitation, temperature corrections, and the simulation of glacier dynamics. On the other hand, in the Baker catchment, there are currently no estimations of glacier runoff contributions.

These three catchments allow us to make comparisons with our regional simulations at the Andes scale using consistent data (e.g., corrected climate datasets and glacier outlines) and methods (e.g., simulating mass balance, dynamics, and glacier runoff), update previous results, and provide new glacier runoff estimates. For example, it is necessary to understand what occurs during the prolonged dry period in central Chile and Argentina. In addition, river discharge records were collected from Soruco et al. (2015) and the CAMELS-CL project (Alvarez-Garreton et al., 2018) for Bolivia and Chile, respectively. In Bolivia, we considered the four glacierized head catchments providing water to the La Paz catchment: Tuni-Condoriri, Milluni, Hampaturi, and Incachaca (discharge records from 2001 to 2007) with a total surface area of 227 km<sup>2</sup> and 7.5 % of the glacierized surface area (mean elevation of 5019 m a.s.l.). In Chile, for the Maipo catchment, we compiled records from Río Maipo at the El Manzano station (catchment id: 5710001; 4839 km<sup>2</sup>; discharge records from 1990 to 2019) and Río Mapocho at the Los Almendros catchments (catchment id: 5722002; 638 km<sup>2</sup>; discharge records from 1990 to 2019) with a glacierized surface area of 7.5 % (mean elevation of 4259 m a.s.l.). For the Baker catchment, we used the Río Baker Bajo Ñadis records (catchment id: 11545000; 27 403 km<sup>2</sup>; discharge records from 2004 to 2019), considering a glacierized surface area of 8.2 % (mean elevation of 1612 m a.s.l.). Note that only the glacier runoff contribution will be simulated.

## 2.2 OGGM details

We ran the OGGM model (Maussion et al., 2019) for each glacier and then the results per catchment were aggregated for each of the 786 catchments across the Andes (including the three selected test catchments for a detailed analysis). OGGM is a modular and open-source numerical workflow implemented in Python that provides preprocessed datasets, such as DEMs, glacier hypsometry, and glacier flowlines, that can be used to explicitly simulate glacier mass balance and ice dynamics using calibrated parameter values for each glacier. Here, we ran OGGM from level 2, comprising the flowlines and their downstream lines. However, we used a new baseline climate time series (corrected TerraClimate) as input data. We also calibrated the mass balances and the bed inversion (ice thickness) which allowed us to obtain hydrological outputs (glacier runoff) (details at <https://docs.oggm.org/en/v1.4.0/input-data.html>, last access: July 2022). The spatiotemporal configuration of the model used in this study is at the glacier scale and at the monthly time step. The simulation results were analyzed at different spatial scales: by glacierized catchment, glaciological zone, and regionally.

The required input data for running the model are as follows: air temperature and precipitation time series, as well as glacier outlines and surface topography for specific years.

From these input data we computed annual simulated processes such as the surface mass balance, glacier volume and area, monthly glacier melt (snow and ice), and rainfall on glaciers (Fig. 1). Modeled processes, such as the surface mass balance and glacier volume, were calibrated (Fig. 2; Table 1). The calibration procedure of the parameters was applied per glacier to match the simulated mass balance of 2000–2019 to the geodetic mass balance product from Hugonnet et al. (2021). The simulated glacier volume was calibrated using the Farinotti et al. (2019) product at a glaciological zone scale to fit the Glen A parameter. In other words, the same Glen A parameter was used for each glaciological zone.

First, using a glacier outline and topography, OGGM estimates the flow lines and catchments per glacier, and then the flow lines are calculated using a geometrical algorithm (adapted from Kienholz et al., 2014). Assuming a bed shape, it estimates the ice thickness based on mass conservation and shallow-ice approximation (Farinotti et al., 2009; Maussion et al., 2019). After these numerical steps, it is possible to determine the area and volume per glacier. The mass balance is implemented using a precipitation phase partitioning and a temperature-index approach (Braun and Renner, 1992; Hock, 2003; Marzeion et al., 2012). The monthly mass balance  $mb_i$  at an elevation  $z$  is calculated as follows:

$$mb_i(z) = TC_{p_i}^{snow}(z) \cdot P_f - M_f \cdot \max(cTC_{t_i}(z) - T_{melt}, 0), \quad (3)$$

where  $TC_{p_i}^{snow}$  is the TerraClimate solid precipitation before being scaled by the precipitation correction factor ( $P_f$ ),  $M_f$  is the glacier's temperature melt factor, and  $cTC_{t_i}$  is the monthly corrected TerraClimate temperature.  $P_f$  and  $M_f$  parameters are related to the snow/ice onset ( $T_{melt}$ ) and precipitation fraction ( $T_i^{snow}$  and  $T_i^{rain}$ ). Their values are different across the Andes.  $T_{melt}$  is the monthly air temperature above which snow/ice melt is assumed to occur (0 °C for the Dry and Wet Andes and 2.1 °C for the tropical Andes).  $T_i^{snow}$  is calculated as a fraction of the total precipitation ( $cTC_p$ ) where 100 % is obtained if  $cTC_{t_i} \leq T_i^{snow}$  (0 °C for the Dry and Wet Andes and 2.1 °C for the tropical Andes) and 0 % if  $cTC_{t_i} \geq T_i^{rain}$  (2 °C for the Dry and Wet Andes and 4.1 °C for the tropical Andes), using a linear regression between these temperature thresholds to obtain the solid and liquid precipitation fraction. Here,  $M_f$  was calibrated for each glacier individually using the previously described glacier volume change datasets (Hugonnet et al., 2021). The calibrated parameter values are summarized by glaciological zone in Table 1.

### 2.2.1 Model setup, calibration, and validation

The input data are as follows: the corrected monthly TerraClimate precipitation ( $cTC_p$ ) and temperature ( $cTC_t$ ), glacier outlines were obtained from RGI v6.0 (RGI Consortium, 2017), assuming the glacier outlines of all glaciers were made for the year 2000. The surface topography data were

**Table 1.** Calibrated parameter values used in the glacier mass balance and volume simulations across the Andes (11° N to 55° S) during the period 2000–2019.

| Region         | Zone | Mass balance parameter values           |                             |  |                                    |  |  | Volume parameter  |
|----------------|------|---|-----------------------------|--|------------------------------------|--|--|---|
|                |      | Temperature LR<br>[°C m <sup>-1</sup> ] | Precipitation factor<br>[-] | Mean melt factor<br>[mm mth <sup>-1</sup> °C <sup>-1</sup> ] | Temperature for melt onset<br>[°C] | Temperature at start of snowfall<br>[°C] | Temperature at start of rainfall<br>[°C] | Glen A inversion<br>[s <sup>-1</sup> Pa <sup>-3</sup> ] |
| Tropical Andes | IT*  |   |                             | 434  |                                    |  |  | $2.4 \times 10^{-23}$                                   |
|                | OT2* | -0.0066                                 | 1                           | 284  | 2.1                                | 2.1                                      | 4.1                                      | $6.3 \times 10^{-24}$                                   |
|                | OT3* |   |                             | 432  |                                    |  |  | $1.2 \times 10^{-23}$                                   |
| Dry Andes      | DA1  | -0.0082                                 | 2.8                         | 418  |                                    |  |  | $2.4 \times 10^{-25}$                                   |
|                | DA2  | -0.0065                                 | 1.9                         | 479  |                                    |  |  | $1.3 \times 10^{-23}$                                   |
|                | DA3  | -0.0063                                 | 4                           | 299  |                                    |  |  | $2 \times 10^{-24}$                                     |
|                | WA1  |   |                             | 103  | 0                                  | 0  | 2  | $1.7 \times 10^{-23}$                                   |
|                | WA2  | -0.0051                                 | 4                           | 118  |                                    |  |  | $1.9 \times 10^{-23}$                                   |
| Wet Andes      | WA3  |   |                             | 152  |                                    |  |  | $6 \times 10^{-24}$                                     |
|                | WA4  | -0.0063                                 | 2.3                         | 128  |                                    |  |  | $1.3 \times 10^{-23}$                                   |
|                | WA5  |   |                             | 179  |                                    |  |  | $1 \times 10^{-23}$                                     |
|                | WA6  |   |                             | 139  |                                    |  |  | $1.5 \times 10^{-23}$                                   |

\* Related to zones of the tropical Andes region: inner tropics (IT) and outer tropics (OT2 and OT3).

sourced from NASADEM (Crippen et al., 2016). NASADEM has a spatial resolution of 1 arcsec ( $\sim 30$  m), and the data were acquired in February 2000 (NASA JPL, 2020). The simulated glacier volume was calibrated using the Farinotti et al. (2019) product at a glaciological zone scale to fit the Glen A parameter (Fig. 2; Table 1).

Lastly, the simulated mass balance was evaluated in comparison with in situ mass balance observations (Marangunic et al., 2021; WGMS, 2021). Although the OGGM outputs are in calendar years and the observations are in hydrological years, we consider it essential to evaluate the interannual performance (Pearson correlation,  $p$  value, variance, RMSE, and bias from average difference) and the cumulative mass balance since the year 2000.

### 3 Results

#### 3.1 Climatic variations on glaciers across the Andes during the period 2000–2019

The climate associated with 786 Andean glacierized catchments (11° N to 55° S) presents a mean corrected TerraClimate temperature ( $cTC_t$ ) of  $-0.2 \pm 2.2$  °C and a mean annual corrected TerraClimate precipitation ( $cTC_p$ ) of  $2699 \pm 2006$  mm yr<sup>-1</sup> between 2000 and 2019. The various glaciological regions show significant climatic differences, with contrasting extreme values between the tropical Andes and Wet Andes in terms of mean annual precipitation ( $939 \pm 261$  and  $3751 \pm 1860$  mm yr<sup>-1</sup>, respectively) and also mean annual temperature between the Dry Andes and tropical Andes ( $-3.7 \pm 1.4$  °C and  $1.3 \pm 0.8$  °C, respec-

tively). Certain glaciological zones highlight very negative and positive mean annual temperature values such as Dry Andes 2 ( $-4.8$  °C) and Wet Andes 2 ( $1.9$  °C), as well as lower and higher cumulative precipitation values such as Dry Andes 1 ( $447$  mm yr<sup>-1</sup>) and Wet Andes 5 ( $6075$  mm yr<sup>-1</sup>). Meanwhile, variations in climate between the periods 2000–2009 and 2010–2019 across the Andes show a cumulative precipitation decrease of  $-9\%$  ( $-234$  mm yr<sup>-1</sup>) and a mean annual temperature increase of  $0.4 \pm 0.1$  °C. Between these two periods, precipitation decreases primarily in the Dry Andes ( $-256$  mm yr<sup>-1</sup>;  $-23\%$ ) and Wet Andes ( $-337$  mm yr<sup>-1</sup>;  $-9\%$ ), and increases in the tropical Andes ( $44$  mm yr<sup>-1</sup>;  $5\%$ ), whereas the temperature increases between  $0.3$  and  $0.4$  °C in all regions. At the glaciological zone scale, only the tropical Andes and Dry Andes 1 ( $12\%$ ) show a cumulative increase in precipitation, whereas a larger decrease in precipitation is found in Dry Andes 2 ( $-32\%$ ) and Dry Andes 3 ( $-27\%$ ). The mean annual temperature increases in all zones, especially the inner tropics ( $+0.6$  °C) followed by Wet Andes 3 ( $+0.5$  °C). A summary of the variations in climate by glaciological zone is presented in Table 2.

Our  $cTC_t$  evaluation is statistically significant ( $p < 0.01$ ) at 32 meteorological stations with a mean temperature bias of  $0.4$  °C and a mean correlation of  $0.96$ . These results are available in Fig. S2 and Table S2. The regional results show a larger bias in the tropical Andes (mean =  $2.1$  °C for four stations) with a meteorological station mean elevation of  $4985$  m a.s.l., where  $cTC_t$  cannot represent the mean monthly temperature. However,  $cTC_t$  represents well the maximum temperatures in spring/summer and the minimum temperatures in winter. The lowest bias is observed in the Wet An-

**Table 2.** Mean annual changes in glacier area and volume, glacier runoff, and climate between the periods 2000–2009 and 2010–2019 at the glaciological zone scale across the Andes (11° N to 55° S).

| Region         | Zone | Change in surface area [km <sup>2</sup> ] (%) | Change in volume [km <sup>3</sup> ] (%) | Change in glacier melt [m <sup>3</sup> s <sup>-1</sup> ] (%) | Change in rainfall on glaciers [m <sup>3</sup> s <sup>-1</sup> ] (%) | Simulated area [km <sup>2</sup> ] and percentage in total glacierized area (%) | cTC <sub>t</sub> change [°C] | cTC <sub>p</sub> change [mm yr <sup>-1</sup> ] (%) |
|----------------|------|---|---|--|--|--|------------------------------|--|
| Tropical Andes | IT   | -5.8 (-3)                                     | -0.7 (-8)                               | 4.1 (73)   | 0.4 (74)   | 191 (88)   | 0.6                          | 81 (7.1)   |
|                | OT2  | -19.3 (-4)                                    | -1.2 (-8)                               | 2.8 (23)   | 0.3 (10)   | 437 (77)   | 0.3                          | 19 (1)   |
|                | OT3  | -30.4 (-3)                                    | -4 (-7)                                 | 14.1 (40)  | 1.6 (25)   | 1149 (81)  | 0.4                          | 43 (5.2)   |
| Dry Andes      | DA1  | -5.2 (-2)                                     | -0.4 (-4)                               | 1.8 (62)   | 0.2 (106)  | 218 (93)   | 0.3                          | 50 (11.9)  |
|                | DA2  | -7.4 (-1)                                     | -2 (-4)                                 | 11.3 (59)  | 0.1 (14)   | 770 (76)   | 0.3                          | -269 (-32)   |
|                | DA3  | -32.6 (-5)                                    | -3 (-8)                                 | 8.5 (23)   | -0.1 (-3)  | 613 (97)   | 0.3                          | -629 (-27.2)                                       |
| Wet Andes      | WA1  | -7 (-3)                                       | -1.1 (-8)                               | 1.7 (6)  | -1.6 (-13)   | 237 (93)   | 0.3                          | -937 (-18.3)                                       |
|                | WA2  | -41.2 (-3)                                    | -11.6 (-13)                             | 10.7 (6)   | -11.7 (-9)   | 1550 (91)  | 0.4                          | -454 (-8)  |
|                | WA3  | -4.9 (-1)                                     | -3 (-7)                                 | 4.4 (14)   | 1.1 (5)  | 469 (4)  | 0.5                          | -161 (-4.4)  |
|                | WA4  | -72 (-2)                                      | -21.4 (-9)                              | 15.3 (8)   | 4.4 (5)  | 3746 (57)  | 0.4                          | -96 (-5.1)   |
|                | WA5  | 4.5 (1)                                       | -0.3 (-1)                               | 4.1 (14)   | 2.1 (7)  | 378 (15)   | 0.4                          | -407 (-6.5)  |
|                | WA6  | -23.9 (-2)                                    | -10.5 (-8)                              | 7.7 (7)  | -4.5 (-5)  | 1524 (32)  | 0.3                          | -382 (-10)   |

des and Dry Andes. The Wet Andes, with a meteorological station mean elevation of 813 m a.s.l., shows good results in terms of reproducing the mean monthly temperature in most stations, with a minimum correlation higher than 0.86. In the Dry Andes, with a meteorological station mean elevation of 3753 m a.s.l. (18 stations) and bias of 0.2 °C, the cTC<sub>t</sub> reproduces the mean monthly temperature very well. However, in some stations, such as La Frontera and Estrecho Glacier (29° S), the mean cTC<sub>t</sub> is warmer than 6 °C, whereas in other stations, such as El Yeso Embalse (33.7° S) and Cipreses glacier (34.5° S), the mean cTC<sub>t</sub> is colder than 6 °C. (The detailed cTC<sub>t</sub> evaluation based on bias and Pearson's correlation can be found in Fig. S2 as well as Tables S1 and S3.) The cTC<sub>t</sub> presented a mean bias of 2.1 °C in the tropical Andes and a mean bias of 0.2 °C in the Dry Andes and Wet Andes in comparison with in situ measurements.

### 3.2 Glaciological changes across the Andes during the period 2000–2019

The 36 % of the total glacierized surface area across the Andes (11° N to 55° S) is simulated to obtain the annual glacier area and glacier volume, as well as the monthly glacier runoff (glacier melting and rainfall on glaciers).

Considering mean values for the periods 2000–2009 and 2010–2019, the glacier volume and surface area in the Andean catchments show a decrease of -8.3 % (-59.1 km<sup>3</sup>) and -2.2 % (-245 km<sup>2</sup>), respectively. This corresponds to a mean annual mass balance difference between the two periods of  $-0.5 \pm 0.3$  m w.e. yr<sup>-1</sup> (Fig. 2d). A decrease in glacier volume and surface is seen in 93 % of the catchments ( $n = 724$ ), whereas 7 % of the catchments ( $n = 65$ ) present an increase in glacier volume and surface. The loss in glacier

volume (Fig. 2b) is largest (-47.8 km<sup>3</sup>, -9 %) in the Wet Andes, followed by the tropical Andes (-5.9 km<sup>3</sup>, -7 %) and Dry Andes (-5.4 km<sup>3</sup>, -6 %). Similarly, a larger decrease in the glacier surface area (Fig. 2c) is observed in the Wet Andes (-144.4 km<sup>2</sup>, -2 %), followed by the tropical Andes (-55.5 km<sup>2</sup>, -4 %) and lastly the Dry Andes (-45.2 km<sup>2</sup>, -3 %). As expected, the correlation between both glacier change variables is consistent at the zone scale, showing a positive correlation between the changes in area and volume ( $r = 0.9$ ).

When estimating the mass balance, it is interesting to check the calibrated melt factors ( $M_f$ ) of the temperature-index model in order to evaluate its possible regionalization, i.e., to evaluate the spatial coherence (see Fig. 3 and Table 1). The mean calibrated melt factor values decrease from the tropical Andes toward the Wet Andes (tropical Andes:  $0.5 \pm 0.3$  mm h<sup>-1</sup> °C<sup>-1</sup>; Dry Andes:  $0.6 \pm 0.2$  mm h<sup>-1</sup> °C<sup>-1</sup>; Wet Andes:  $0.2 \pm 0.1$  mm h<sup>-1</sup> °C<sup>-1</sup>). The lowest mean temperatures estimated in the Dry Andes imply higher factor values to reach the calibrated mass loss in the few months in which the temperatures exceed 0 °C. The opposite can be observed in the Wet Andes, where low factor values are associated with a greater number of months with temperatures exceeding 0 °C. We obtain very similar values in contiguous zones, with the lowest values found in the Wet Andes (monthly mean below 179 mm °C<sup>-1</sup>), followed by the tropical Andes (monthly mean below 434 mm °C<sup>-1</sup>) and the Dry Andes (monthly mean below 479 mm °C<sup>-1</sup>). The largest melt factor values are found in the Dry Andes where Dry Andes 2 (monthly mean = 479 mm °C<sup>-1</sup>) presents the lowest mean temperatures across the Andes (-4.8 °C between 2000 and 2019). The lowest melting factor values are calibrated in the Wet

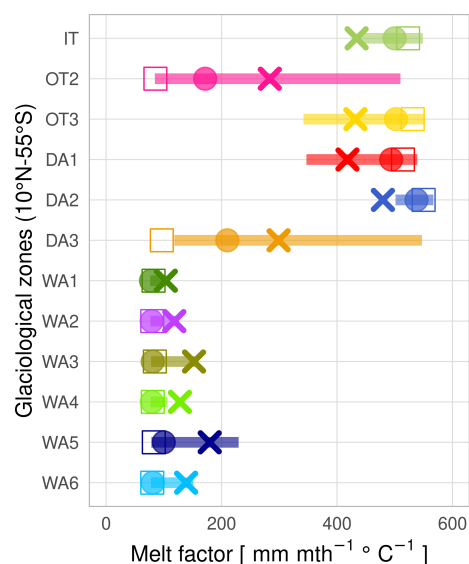


**Figure 3.** Statistics for the calibrated melt factors per glacier at the glaciological zone scale across the Andes. Shown are the mean (×), median (circles), mode (squares), and 25th as well as 75th percentile (lines) values for 13 179 glaciers.

Andes where Wet Andes 1 (monthly mean =  $103 \text{ mm } ^\circ\text{C}^{-1}$ ) shows high mean temperatures ( $1.8^\circ\text{C}$  between 2000 and 2019). Despite this, a lower correlation between the melt factors and mean temperature for the 2000–2019 period is estimated ( $r = -0.5$ ;  $p = 0.08$ ). Conversely, the correlation between the melt factors and mean precipitation for the 2000–2019 period is high ( $r = -0.8$ ;  $p = 0.002$ ).

To test our results we evaluated the simulated mass balance evaluation for the 15 glaciers that can be found in Figs. S3 and S4, as well as Tables S4 and S5. The in situ data show a mean negative mass balance ( $-832 \pm 795 \text{ mm w.e. yr}^{-1}$ ) between 2000 and 2019 greater than our mean simulated mass balance ( $-647 \pm 713 \text{ mm w.e. yr}^{-1}$ ) in the same glaciers. The evaluation results give a mean Pearson correlation of 0.67 (except for the Agua Negra, Ortigas 1, Guanaco, and Amarillo glaciers, for which it shows either no correlation or a negative correlation) with an underestimation of the mean simulated mass balance of  $185 \text{ mm w.e. yr}^{-1}$  (bias); 40% of the glaciers present a correlation equal to or greater than 0.7. In terms of the best results by glaciological region, in the tropical Andes, the Conejeras glacier has a high correlation ( $r = 0.9$ ) and bias ( $1104 \text{ mm w.e. yr}^{-1}$ ), whereas in the Dry Andes, the Piloto Este, Paula, Paloma Este, and Del Rincón glaciers display a high correlation ( $r \geq 0.8$ ) and a mean bias of  $351 \text{ mm w.e. yr}^{-1}$ . In the Wet Andes, the Mocho–Choshuencho and Martial Este glaciers show a moderate correlation ( $r = 0.5$ ) and a lower overestimation of the simulated mass balance ( $-118 \text{ mm w.e. yr}^{-1}$ ). Model limitations are observed on the Zongo glacier ( $r = 0.3$  and bias =  $-224 \text{ mm w.e. yr}^{-1}$ ) in the tropical Andes. In Dry An-

des 1, no correlation is observed in the three monitored glaciers (Guanaco, Amarillo, and Ortigas 1), mainly because sublimation is very high on these glaciers, reaching 81% of the annual ablation (MacDonell et al., 2013). On the other hand, sublimation is lower southward in Dry Andes 2 with 7% of the annual ablation (Ayala et al., 2017). For the tropical zone, sublimation is close to 13% in the outer tropics (Sicart et al., 2005) and 5% in the inner tropics (Favier et al., 2004). However, sublimation is implicitly included in the model through the calibrated melt factor values, which are derived from measured mass balance data by Hugonnet et al. (2021). As a result, our estimates of snow/ice melt in the Dry Andes 1 zone tend to be overestimated.

The details of the glacier changes in the 786 Andean catchments, which are larger in the Wet Andes followed by the tropical Andes and then the Dry Andes, are available in the Supplement.

### 3.3 Changes in glacier runoff across the Andes during the period 2000–2019

Due to glacier changes across the Andes, high glacier runoff variations are observed from glacier melt and rainfall on glaciers (Fig. 4). The mean annual glacier melt in all catchments for the period 2000–2019 was  $696 \text{ m}^3 \text{ s}^{-1}$ . At the regional scale, the Wet Andes shows the largest mean annual glacier melt in the Andes ( $583.5 \text{ m}^3 \text{ s}^{-1}$ ), followed by the Dry Andes ( $59.9 \text{ m}^3 \text{ s}^{-1}$ ) and then the tropical Andes ( $52.7 \text{ m}^3 \text{ s}^{-1}$ ). However, if we look at the mean annual glacier melt changes between the periods 2000–2009 and 2010–2019, we see an increase of 12% ( $86.5 \text{ m}^3 \text{ s}^{-1}$ ) across the Andes, where 84% ( $n = 661$ ) of catchments show an increase and 12% ( $n = 95$ ) of them present a decrease. As Table S6 shows, an increase in glacier melt is observed in catchments with a higher glacier elevation, larger glacier size, lower mean temperature, and higher mean precipitation compared with catchments that show either a decrease in glacier melt or no changes at all. These latter catchments also show the largest decrease in precipitation ( $-10\%$  to  $-14\%$ ).

The mean annual glacier melt changes show the largest percentage increase in the tropical Andes (40%,  $21 \text{ m}^3 \text{ s}^{-1}$ ), followed by the Dry Andes (36%,  $21.7 \text{ m}^3 \text{ s}^{-1}$ ) and the Wet Andes (8%,  $4.8 \text{ m}^3 \text{ s}^{-1}$ ). In addition, significant differences are observed for the different zones: for instance, the inner tropics in the tropical Andes presents the largest increase (73% with only  $4.1 \text{ m}^3 \text{ s}^{-1}$ ), followed by Dry Andes 1 (62% with only  $1.8 \text{ m}^3 \text{ s}^{-1}$ ) in the Dry Andes. In the Wet Andes, the larger percentage of increase in the mean annual glacier melt changes is observed in Wet Andes 5 (14% with  $4.1 \text{ m}^3 \text{ s}^{-1}$ ), showing a lower percentage in comparison with the inner tropics and Dry Andes 1 zones; however, its absolute increase in glacier melt is equal to or greater than  $4.1 \text{ m}^3 \text{ s}^{-1}$ . These results per glaciological zone are summarized in Table 2. Related to the previously described glacier changes (see Sect. 3.2) between the periods 2000–2009 and 2010–

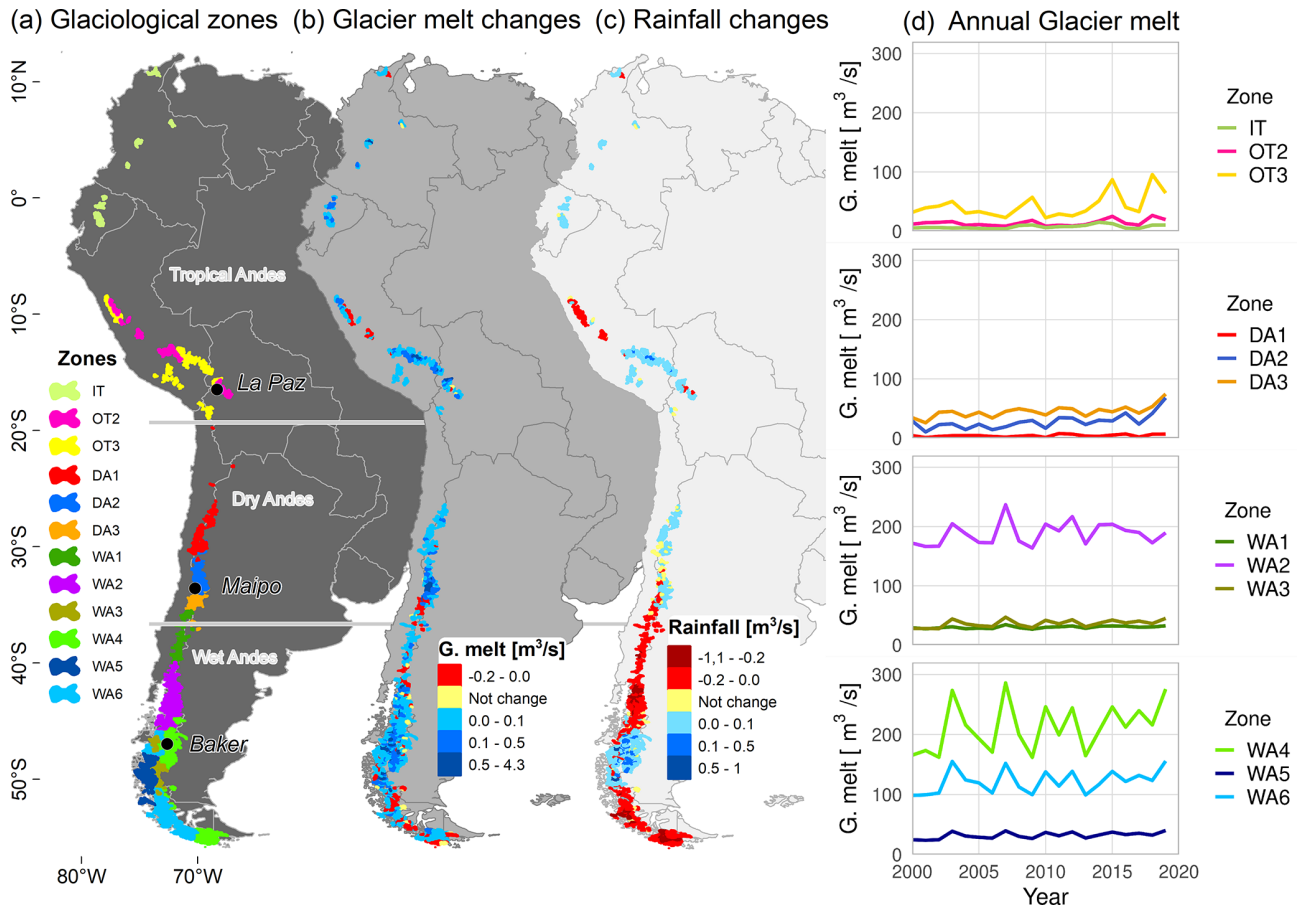


**Figure 4.** Recent glacier runoff components across the Andes. The total glacier melt and rainfall on glaciers represent the mean differences between the periods 2010–2019 and 2000–2009 per catchment ( $n = 786$ ). Panel (a) shows the distribution of the glaciological zones (11° N to 55° S), followed by (b) glacier melt and (c) rainfall on glaciers at the catchment scale. The (d) total annual glacier melt is presented in each glaciological zone. “G. melt” and “Rainfall” refer to changes in (b) glacier melt and (c) rainfall on glaciers, respectively. “G. melt” on the y axis in (d) refers to cumulative annual glacier melt by glaciological zone.

2019, at the glaciological zone scale, we logically find a high negative correlation between the glacier melt and glacier volume changes in the tropical Andes and Dry Andes ( $r = -0.9$ ) as well as the Wet Andes ( $r = -1$ ).

In addition, the mean annual rainfall on glaciers across the Andes is  $387 \text{ m}^3 \text{ s}^{-1}$  for the period 2000–2019. The Wet Andes has the largest amount of annual rainfall ( $372.7 \text{ m}^3 \text{ s}^{-1}$ ), followed by the tropical Andes ( $10.5 \text{ m}^3 \text{ s}^{-1}$ ) and Dry Andes ( $4.2 \text{ m}^3 \text{ s}^{-1}$ ) with the lowest contribution of rainfall.

In terms of the variations in the mean annual rainfall on glaciers between the periods 2000–2009 and 2010–2019, we observe a reduction of  $-2\%$  ( $-7.6 \text{ m}^3 \text{ s}^{-1}$ ) across the Andes, showing a reduction in 41% of the catchments ( $n = 322$ ), whereas the largest proportion of the catchments (51%;  $n = 403$ ) show an increase. Table S6 shows that the catchments with the larger increase in rainfall on glaciers are concentrated in the same latitude range as the catchments with an increase in glacier melt. These catchments have similar glacier elevations and glacier sizes. The catchments that do

not show variations in rainfall on glaciers are concentrated in the Dry Andes region, where the rainfall contributes less to the glacier runoff volume.

At the glaciological region scale, the mean annual rainfall on glaciers decreases in the Wet Andes ( $-3\%$ ,  $10.1 \text{ m}^3 \text{ s}^{-1}$ ) but increases in the tropical Andes (23%,  $2.4 \text{ m}^3 \text{ s}^{-1}$ ) and Dry Andes (3%,  $0.1 \text{ m}^3 \text{ s}^{-1}$ ). In addition, large differences are observed in the glaciological zones (Table 2): e.g., Dry Andes 1 in the Dry Andes has the largest percentage increase (106% with only  $0.2 \text{ m}^3 \text{ s}^{-1}$ ), followed by the inner tropics (74% with only  $0.4 \text{ m}^3 \text{ s}^{-1}$ ) in the tropical Andes. In the Wet Andes, the larger increase (by percent) in the mean annual rain on the glaciers is observed in Wet Andes 5 (6.6% with  $2.1 \text{ m}^3 \text{ s}^{-1}$ ). Other zones, such as Wet Andes 2 and Wet Andes 6, show large absolute reductions ( $-11.7 \text{ m}^3 \text{ s}^{-1}$  and  $-4.5 \text{ m}^3 \text{ s}^{-1}$ , respectively).

The changes in glacier melt and rainfall on glaciers observed in the tropical Andes, Dry Andes, and Wet Andes are

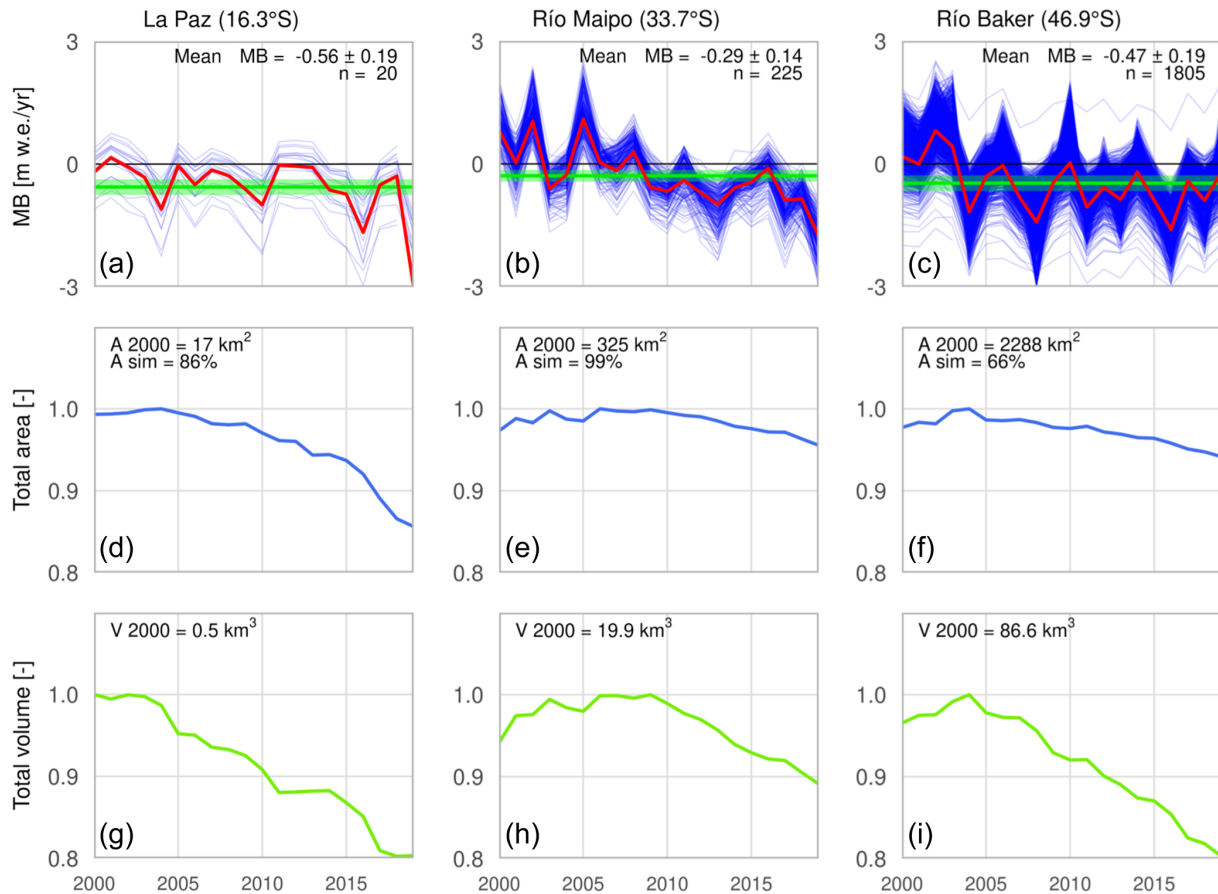


**Figure 5.** Recent annual specific mass balance, surface area, and volume variations in the La Paz, Maipo, and Baker catchments from 2000 to 2019. Panels (a)–(c) show the mass balance for each simulated glacier (blue line), as well as the weighted mean mass balance per catchment (red line). The mean geodetic mass balance and its error for the period 2000–2019 are also presented (green bar). (d–f) presents the total glacierized area per catchment (blue line). The total area from RGI v6.0 and the simulated area percentage are also presented. Panels (g)–(i) exhibit the total volume per catchment (green line). The surface area and volume have both been normalized to make it easier to compare the evolution between the catchments.

summarized in Table 2 and are available, in the Supplement, for the 786 Andean catchments.

### 3.4 Hydro-glaciological behavior at the catchment scale during the period 2000–2019

In this section, we focus on three Andean catchments: La Paz (16° S, tropical Andes), Maipo (33° S, Dry Andes), and Baker (47° S, Wet Andes) (see locations in Figs. 2 and 4), where previous glaciological observations and simulations of glacier evolution and water production have been carried out, and in situ records are also available. Detailed results for each of the 786 catchments and glaciers included are available in the dataset provided in the Supplement.

#### 3.4.1 Glaciological variations in the selected catchments: La Paz (16° S), Maipo (33° S), and Baker (47° S)

Figure 5 shows the annual specific mass balance in the three catchments (2000–2019). The mean over the study period is negative, and there is a negative trend for the annual values toward 2019. For instance, for the Maipo catchment, we estimate a mean annual mass balance of  $-0.29 \pm 0.14 \text{ m w.e. yr}^{-1}$ , a slightly more negative balance in the Baker catchment ( $-0.47 \pm 0.19 \text{ m w.e. yr}^{-1}$ ), and in the glaciers in the La Paz catchment, there is a greater loss of  $-0.56 \pm 0.19 \text{ m w.e. yr}^{-1}$ . In addition, when considering the annual mass balance values, it is possible to note differences between the catchments. The La Paz catchment shows mostly negative annual mass balance values over the whole period, while in the Baker and Maipo catchments the mass balances are predominantly negative after 2004 and 2009, respectively. Considering the total area and vol-

**Table 3.** Hydro-glaciological changes and variations in climate between the periods 2000–2009 and 2010–2019 for the three selected catchments.

| Region | Catchment | Change in surface area [km <sup>2</sup> ] (%) | Change in volume [km <sup>3</sup> ] (%) | Contribution of the annual glacier melt [m <sup>3</sup> s <sup>-1</sup> ] (%) | Contribution of the annual rainfall on glaciers [m <sup>3</sup> s <sup>-1</sup> ] (%) | Total simulated glacierized area [km <sup>2</sup> ] (%) | cTC <sub>t</sub> variation [°C] | cTC <sub>p</sub> variation [mm yr <sup>-1</sup> ] (%) |
|--------|-----------|---|---|---|---|---|---------------------------------|---|
| TA     | La Paz    | -0.96 (-6.7)                                  | -0.1 (-11.5)                            | 0.09 (21.3)   | 0.01 (15.3)   | 14.4 (86)   | 0.5                             | 30 (4)  |
| DA     | Maipo     | -4.2 (-1.3)                                   | -1 (-5)                                 | 4.7 (37)  | 0.02 (2.2)  | 353.9 (99)  | 0.4                             | -454 (-30)  |
| WA     | Baker     | -36.7 (-2.4)                                  | -9.3 (-10.7)                            | 9 (10)  | 4.3 (11.2)  | 1514 (66)   | 0.5                             | -52 (-2)  |

ume changes per catchment in the periods 2000–2009 and 2010–2019, an overall reduction is observed in each of the three catchments. For the La Paz catchment, considering 86 % (14 km<sup>2</sup>) of glacierized area in 2000 (mean glacierized elevation of 5019 m a.s.l.) and 20 glaciers, the glacierized surface area and volume decrease by -7 % (-1 km<sup>2</sup>) and -11 % (-0.1 km<sup>3</sup>), respectively. For the Maipo catchment, with a larger percentage of simulated glacierized surface area in 2000 (99 %, with mean elevation of 4259 m a.s.l.) and a greater number of glaciers ( $n = 225$ ), the area and volume decrease by -1 % (-4.2 km<sup>2</sup>) and -5 % (-1 km<sup>3</sup>), respectively. For the Baker catchment, which contains the largest glacierized surface area of the three catchments in 2000, we simulated 66 % of this glacierized area (1514 km<sup>2</sup>, with mean elevation of 1612 m a.s.l.) and 1805 glaciers: this area shrank by approximately -2 % (-36.7 km<sup>2</sup>), losing close to -11 % (-9.3 km<sup>3</sup>) of its volume. These results are summarized in Table 3.

### 3.4.2 Hydrological contribution of glaciers in the selected catchments: La Paz (16° S), Maipo (33° S), and Baker (47° S)

The La Paz, Maipo, and Baker catchments display large climatic and glaciological differences over the period 2000–2019. For instance, contrasting cumulative precipitation amounts can be found between the Baker and La Paz catchments ( $2224 \pm 443$  and  $791 \pm 100$  mm yr<sup>-1</sup>, respectively), while the La Paz and Maipo catchments present the maximum difference in mean annual temperature ( $1.4 \pm 0.5$  °C and  $-4.1 \pm 0.5$  °C, respectively) (Fig. 6). At a seasonal scale, precipitation in the Maipo and Baker catchments is concentrated in fall and winter (April to September), even if the latter catchment also has a significant amount of precipitation in summer. Conversely, precipitation in the La Paz catchment mainly occurs in spring and summer (October to March). In addition, the La Paz and Baker catchments are characterized by the warmest temperatures (> 0 °C) in spring and summer; the warmest temperatures for the Maipo catchment occur in summer. Variations in the climatic conditions are observed between 2000–2009 and 2010–2019. For instance, a decrease in cumulative precipitation is observed in

the Maipo (-30 %; -454 mm yr<sup>-1</sup>) and Baker catchments (-2 %; -52 mm yr<sup>-1</sup>), but an increase can be seen in the La Paz catchment (4 %, 30 mm yr<sup>-1</sup>). The mean annual temperature increases in the three catchments (+0.5 °C in La Paz and Baker, +0.4 °C in Maipo).

The glacier runoff simulation, which considers the glacier melt (ice melt and snowmelt) and rainfall on glaciers (liquid precipitation), shows strong differences between the catchments (Fig. 6). Over the period 2000–2019, the glaciers in the Baker catchment have the highest mean annual glacier melt ( $94 \pm 19.6$  m<sup>3</sup> s<sup>-1</sup>), followed by those in the Maipo ( $15.1 \pm 4.2$  m<sup>3</sup> s<sup>-1</sup>) and La Paz catchments ( $0.5 \pm 0.2$  m<sup>3</sup> s<sup>-1</sup>). The rainfall on glaciers contributes 30 % to glacier runoff in the Baker catchment ( $41 \pm 10.1$  m<sup>3</sup> s<sup>-1</sup>); a lower value is found in the La Paz catchment with 17 % ( $0.1$  m<sup>3</sup> s<sup>-1</sup>) followed by the Maipo catchment with 5 % ( $0.8 \pm 0.3$  m<sup>3</sup> s<sup>-1</sup>), which is the lowest contribution of rainfall on glaciers in these catchments. The simulations of glacier runoff changes between the periods 2000–2009 and 2010–2019 for the three catchments show an increase in glacier melt and rainfall on glaciers. The largest relative increase in mean annual glacier melt is observed in the Maipo catchment with 37 % ( $4.7$  m<sup>3</sup> s<sup>-1</sup>), followed by the La Paz catchment with 21 % ( $0.09$  m<sup>3</sup> s<sup>-1</sup>) and the Baker catchment with 10 % ( $9$  m<sup>3</sup> s<sup>-1</sup>). Meanwhile, the largest relative increase in the mean annual rainfall on glaciers is observed in the La Paz catchment (15 %;  $0.01$  m<sup>3</sup> s<sup>-1</sup>), followed by the Baker catchment (11 %;  $4.3$  m<sup>3</sup> s<sup>-1</sup>) and lastly the Maipo catchment (2 %;  $0.02$  m<sup>3</sup> s<sup>-1</sup>). The results for the glacier melt and rainfall on glaciers are summarized in Table 3.

In Fig. 7, at a mean monthly temporal scale for the period 2000–2019, the glacier melt simulation presents a short maximum during summer (January to February) in the Maipo and Baker catchments. In contrast, peaks in the La Paz catchment are extended during spring and summer (November to March) highlighting the so-called transition season (between September and November) where there is a low amount of rainfall on glaciers and glacier melt progressively increases. In the Baker catchment, melting begins earlier in September, while in Maipo it begins later (November). The interannual variability in glacier melt over the periods 2000–2009 and 2010–2019 shows a larger contribution from the glacier

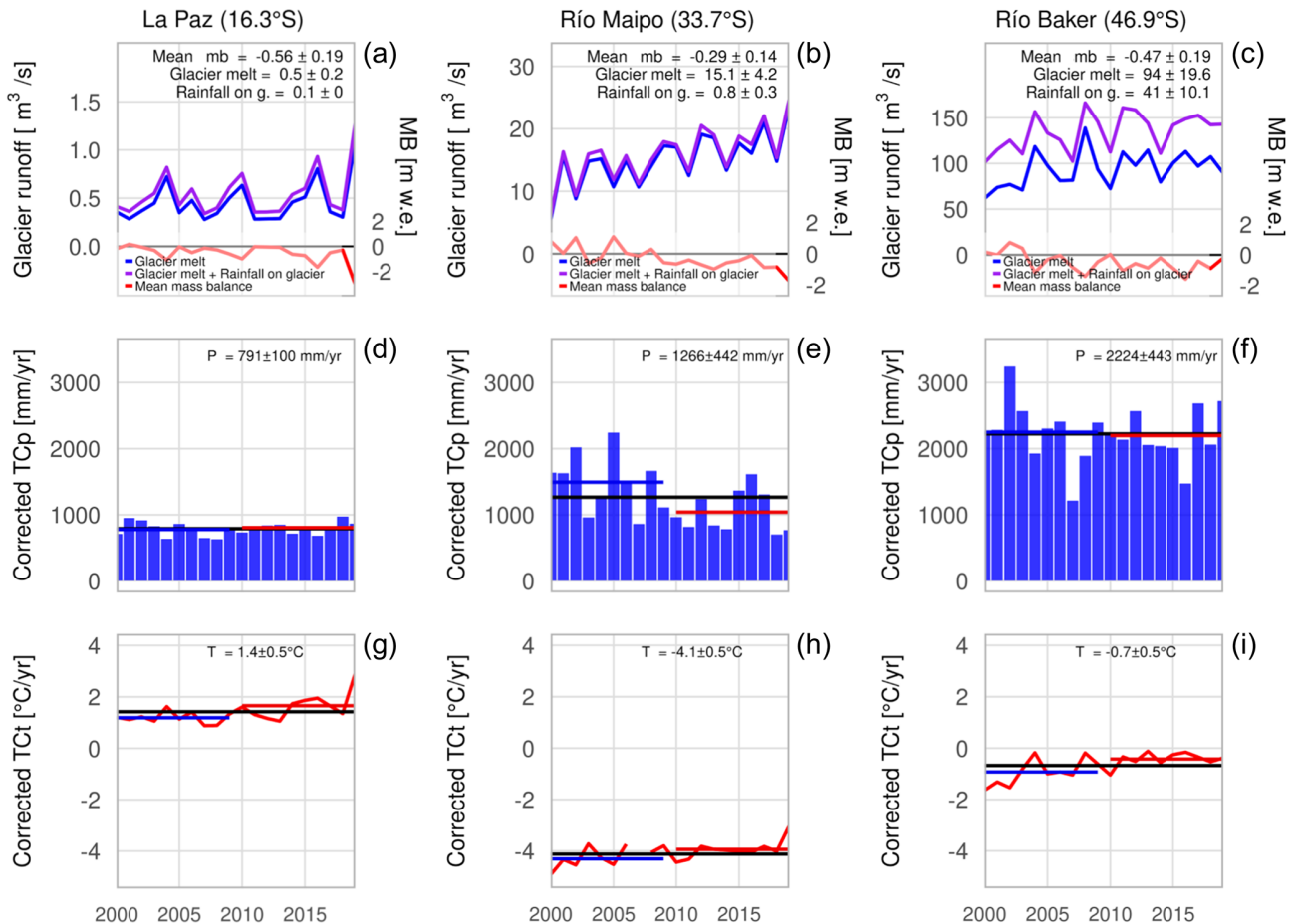


**Figure 6.** Hydro-glaciological responses and climate variations in the La Paz, Maipo, and Baker catchments from 2000 to 2019. The first row (a–c) presents the mean annual glacier runoff (purple line = ice melt + snowmelt + rainfall on glaciers), the mean annual glacier melt (blue line = ice melt + snowmelt), and the annual specific mass balance (red line). The other rows (d–i) show the mean total annual precipitation and mean annual temperature with the mean annual amount for the periods 2000–2019 (black line), 2000–2009 (blue line), and 2010–2019 (red line).

in the period 2010–2019 for the Maipo catchment. Furthermore, the simulated rainfall on glaciers is larger mainly during the summer season in all catchments, with more rainfall in the La Paz catchment (December to February) after the transition season.

For the mean annual discharge measurements in each catchment and the mean annual simulated glacier runoff (glacier melt and rainfall on glaciers) between 2000 and 2019 (Fig. 8), we estimate that the largest glacier runoff contribution is in the Baker catchment (24%), followed by the La Paz (22%) and Maipo catchments (14%), where all catchments present a similar proportion of glacierized surface area (7.5%–8.2%). If we consider the summer season only (January to March), the glacier runoff contribution is highest in the Baker catchment (43%), followed by the Maipo (36%) and La Paz catchments (18%), where the larger percentage of glacier melt is found in the Maipo catchment (34%) and the larger percentage of rainfall on glaciers

is displayed in the Baker catchment (12%). Unlike the Maipo and Baker catchments, which present a maximum glacier runoff contribution in the summer season, the La Paz catchment shows the largest glacier runoff contribution (45%) in the transition season (September to November).

## 4 Discussion

### 4.1 Comparison with previous studies across the Andes

Huss and Hock (2018) studied 12 Andean catchments across the Andes (1980–2000 and 2010–2030) and estimated an increase in glacier runoff in the tropical Andes (Santa and Titicaca catchments) and the Dry Andes (Rapel and Colorado catchments). Our results are consistent with these estimates. We show an increase in glacier melt of 40% and 36% in both regions, respectively, between the periods 2000–2009 and 2010–2019. However, in the Wet Andes, Huss and Hock

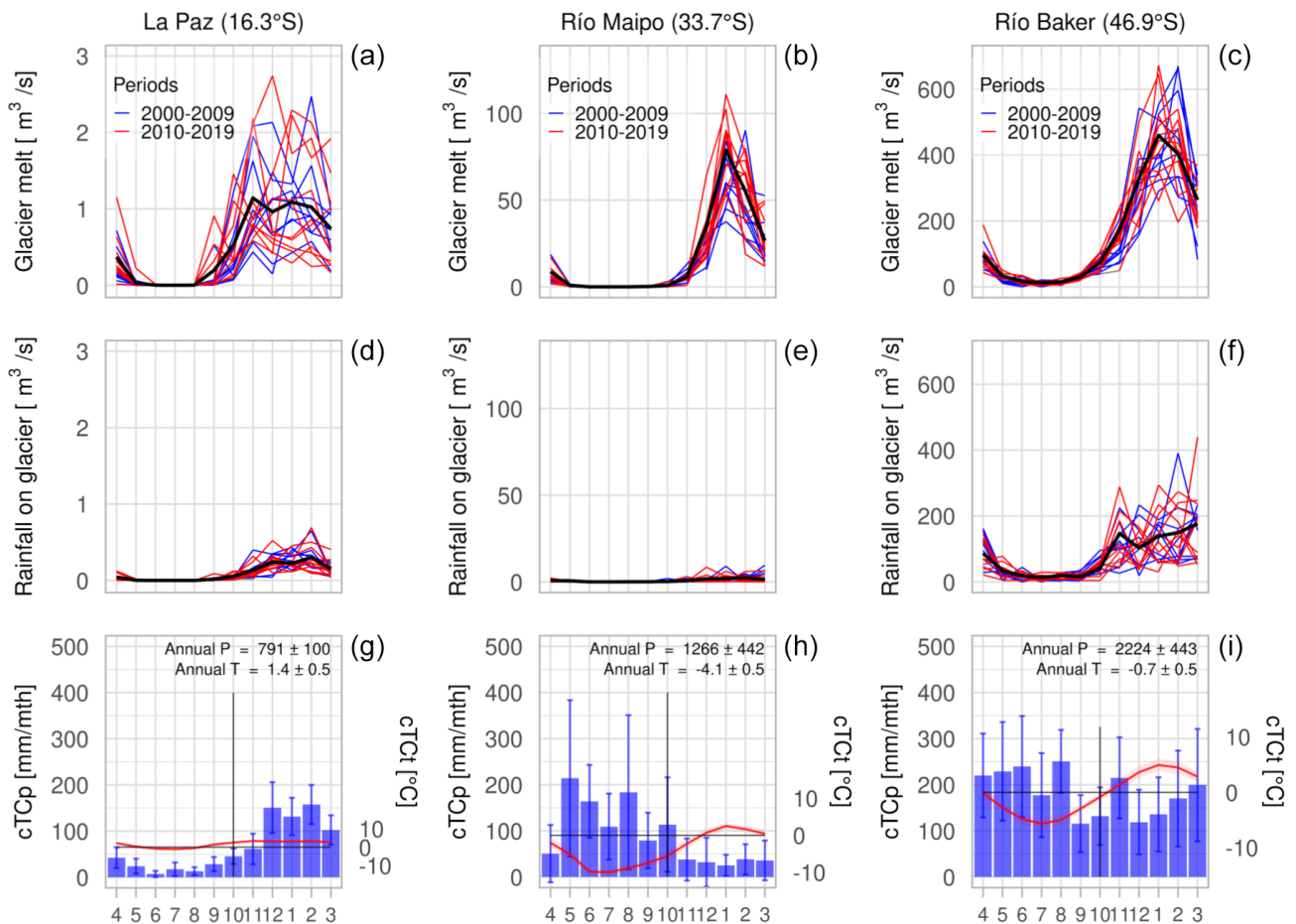


**Figure 7.** Monthly hydro-glaciological responses and climate variations in the La Paz, Maipo, and Baker catchments from 2000 to 2019. The first (a–c) and second (d–f) rows present the mean monthly glacier melt and rainfall on glaciers (black line) and the mean amounts per year during the periods 2000–2009 (red lines) and 2010–2019 (blue lines). In the last row (g–i), the climographs show the mean monthly precipitation (blue bars) and temperature (red line) for the period 2000–2019.

(2018) did not estimate any changes in glacier runoff on the western side of the Andes (Biobio catchment), and instead found a decrease (Río Negro catchment) and an increase (Río Santa Cruz catchment) in glacier runoff on the eastern side of the Andes. Our results for this region show an increase in glacier melt of 8 % and a decrease in rainfall on glaciers of –3 %.

Based on local reports in the tropical Andes, the catchment associated with the Los Crespos glacier (catchment id: 6090223080) on the Antisana volcano shows a small decrease in the glacier area of –1 % between the periods 2000–2009 and 2010–2019, which is in agreement with Basantes-Serrano et al. (2022). Their study estimated that almost half of the glacier area (G1b, G2-3, G8, G9, and G17) had a positive mass balance during the period 1998–2009 with the largest glacier presenting a mass balance of  $0.36 \pm 0.57 \text{ m.w.e. yr}^{-1}$ , in agreement with our mass balance estimation at the catchment scale of  $0.2 \pm 0.5 \text{ m.w.e. yr}^{-1}$  (2000–2009). However, in this region, the corrected Terr-

aClimate temperature cannot reproduce the magnitude of the monthly temperature variation (see Fig. S2). This limits the effectiveness of the parameter values used in the model to accurately simulate the melting onset and the amount of solid and liquid precipitation. Furthermore, the mass balance simulation is performed through the temperature-index model which does not take the sublimation process into account; and in addition, it runs at a monthly time step thereby limiting the relevant processes that occur hourly. On the other hand, the catchments that contain the Zongo glacier (catchment id: 6090629570) and the Charquini glacier (catchment id: 6090641570) display results that are consistent with the observations of others (Rabatel et al., 2012; Seehaus et al., 2020; Autin et al. 2022). In addition, our simulated mass balance evaluation on the Zongo glacier shows a low bias ( $-0.2 \text{ m.w.e. yr}^{-1}$ ) with regard to the observations. In the Dry Andes, the catchments associated with the Pascua Lama area (catchment id: 6090836550 and catchment id: 6090840860), the Tapado glacier (catch-

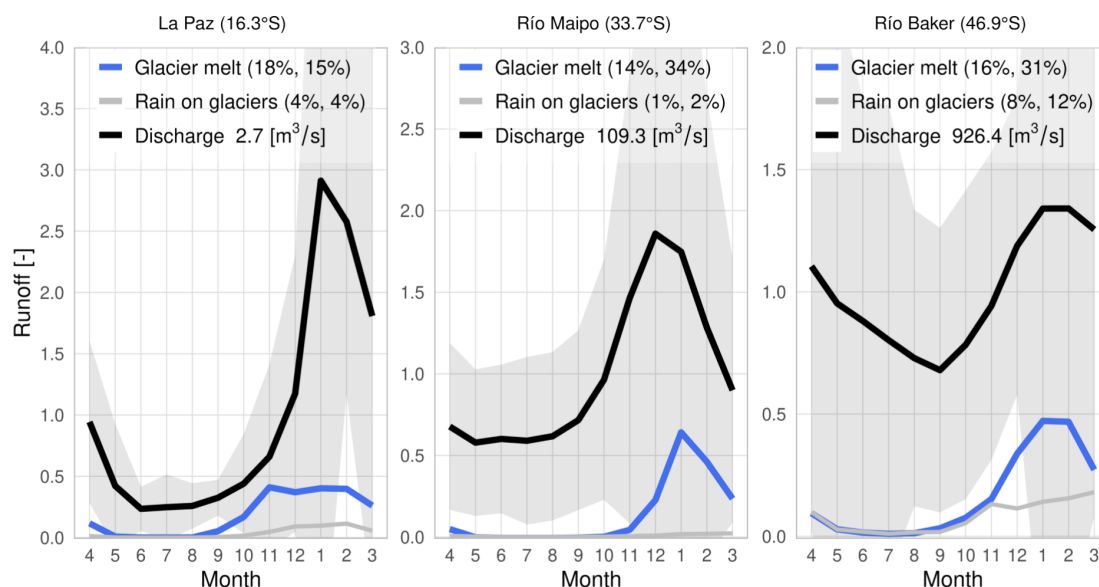


**Figure 8.** Monthly simulated glacier runoff (glacier melt + rainfall on glaciers) and discharge measurements in the La Paz, Maipo, and Baker catchments from 2000 to 2019. The results for the glacier melt (blue lines) and rainfall on glacier calculations (gray lines) are presented, as well as the discharge measurement (black line) and its standard deviation (gray area). The mean annual glacier runoff contribution (as a percentage) and the mean glacier runoff contribution (as a percentage) from January to March are shown in parentheses. The values are normalized by the mean river discharge.

ment id: 6090853340), and the glaciers of the Olivares catchment (catchment id: 6090889690) show consistent results in terms glaciological variations in comparison with the observations (Rabatel et al., 2011; Malmros et al., 2016; Farías-Barahona et al., 2020; Robson et al., 2022). In the Wet Andes, the catchments associated with the Chilean side of the Monte Tronador (catchment id: 6090945100) and the Martial Este and Alvear glaciers in Tierra del Fuego (catchment id: 6090037770) show results that are consistent with previous reports (Rabassa 2010; Ruiz et al., 2017). Despite this, it is possible that our methodology could overestimate precipitation in some catchments; for example, the cumulative precipitation associated with the Nevados de Chillán catchment (catchment id: 6090916140) was estimated at  $4023 \text{ mm yr}^{-1}$ .

At the glaciological region scale, previous studies have reported a large decrease in the percentage of glacier area in the tropical Andes of  $-29\%$  (2000–2016) (Seehaus et al., 2019, 2020), followed by the Dry Andes between  $-29\%$  and  $-30\%$  (Rabatel et al., 2011; Malmros et al., 2016) although for a longer time period. In the Wet Andes, Meier et al. (2018) reported a  $-9\%$  decrease in the glacier area (1986–2016). Our simulations are consistent with these observed glacier area reductions. In addition, Caro et al. (2021) estimated a similar trend across the Andes between 1980 and 2019 (tropical Andes:  $-41\%$ ; Dry Andes:  $-39\%$ ; Wet Andes:  $-24\%$ ). On the other hand, we found high correlations between the mean annual climatic variables and annual mass balance. In the Dry Andes, this correlation was high with precipitation ( $r = 0.8 \pm 0.1$ ;  $p < 0.05$ ), and in the

Wet Andes, temperature was correlated with mass balance ( $r = -0.7 \pm 0.1$ ;  $p < 0.05$ ) as previously observed by Caro et al. (2021). These correlations between precipitation or temperature with the annual mass balances for each catchment across the Andes can be reviewed in Fig. S5 and Table S7.

#### 4.2 Comparison of our results with previous studies in the three selected catchments

In the La Paz catchment, Soruco et al. (2015) evaluated the mass balance of 70 glaciers (1997–2006) and their contribution to the hydrological regime. In the present study, we simulated a less negative mass balance ( $-0.56 \pm 0.19 \text{ m w.e. yr}^{-1}$  vs.  $-1 \text{ m w.e. yr}^{-1}$ ) considering a larger glacierized area due to the use of RGI v6.0 (with  $14.1 \text{ km}^2$  in comparison with  $8.3 \text{ km}^2$ ). Our estimation of the mean annual glacier runoff (22%) is larger than the previous estimation close to 15% (Soruco et al., 2015). This may be due to the fact that we have considered a warmer 2010–2019 period than the one observed in Soruco et al. (2015). Unlike the previous report, we estimated a larger glacier runoff contribution during the wet season (26% from October to March) and increasing in the transition season (45% from September to November). This increase in glacier runoff contribution given by the model agrees with the larger glacier mass loss observed by Sicart et al. (2007) and Autin et al. (2022) during this season. In the Maipo catchment, we identified a slightly smaller glacierized area ( $325 \text{ km}^2$  for the year 2000;  $-14\%$ ) compared with Ayala et al. (2020) because

they considered rock glaciers from the Chilean glacier inventory. In addition, we observed a more negative mass balance after 2008, coinciding with the mega-drought period characterized by a decrease in precipitation and an increase in temperature (Garreaud et al., 2017). The hydrological response to this negative mass balance trend is an increase in glacier runoff since 2000 that is concentrated between December and March. The modeled mean annual glacier runoff contribution estimation is close to 15 %, reaching 36 % in summer (January to March), and is close to Ayala et al.'s (2020) estimation (16 % at the annual scale for the period 1955–2016). However, this comparison between our results and previous studies in the Maipo and La Paz catchments is limited due to the utilization of different inputs, spatial resolutions, time steps, and workflows in the simulated processes where some processes, such as mass balance of all glaciers, were not done. Lastly, in the Baker catchment, Dussailant et al. (2012) stated that catchments associated with the Northern Patagonian Icefield (NPI) are strongly conditioned by glacier melting. In this respect, Huss and Hock (2018) did not identify glacier runoff changes between the periods 1980–2000 and 2010–2030 – they only considered 183 km<sup>2</sup> of the glacierized area (–12 % until 2020) – whereas we estimated a 10 % and 11 % increase in glacier melt and rainfall on glaciers, respectively, taking a larger glacierized area (1514 km<sup>2</sup>; –2 % until 2020) into account. The relevance of the rainfall on glaciers with regard to the glacier runoff estimated here is close to 30 % (including glaciers east of the NPI) which is confirmed by Krogh et al. (2014), who estimated that over 68 % of the total precipitation at the catchment scale in the east NPI (León and Delta catchments) corresponds to rainfall.

### 4.3 Simulation limitations

Limitations in the simulations result from different sources: (1) the quality/accuracy of the input data; (2) the calibration of the precipitation and melt factors; and (3) the model itself, including its structure and the processes that are not represented. Regarding the evaluation of the corrected TerraClimate temperature using meteorological observations in the tropical Andes, the corrected TerraClimate data do not reproduce either the low monthly temperature or the higher temperature in specific months which have a mean bias of 2.1 °C (e.g., Llan\_Up-2 9° S, Zongo at glacier station 16° S). These differences found in the corrected TerraClimate data limit the capacity of the ice and snow melting module to accurately simulate the months in which melting can occur. On the other hand, in the Dry Andes and Wet Andes, the corrected TerraClimate temperatures are closer to the in situ observations (mean bias = 0.2 °C) and present a reliable monthly distribution. This results in model parameter values that are in better agreement with the values used in other studies. Other limitations come from RGI v6.0 because some glaciers are considered as only one larger glacier. For example, in the

Dry Andes (catchment id: 6090889690) two large glaciers, the Olivares Gamma and the Juncal Sur, form one (even larger) glacier. These glaciers could underestimate the simulated change in glacier area, limiting the performance of the volume module which depends on the glacier geometry and bedrock shape.

Furthermore, we applied different precipitation factor values in the tropical Andes (1), Dry Andes (1.9–4), and Wet Andes (2.3–4) in order to increase the annual mass balance. These values are in agreement with former studies, for example, similar values were used in the Dry Andes (Masiokas et al., 2016; Burger et al., 2019; Fariás-Barahona et al., 2020). Values that are too high could lead to an overestimation of precipitation on some glaciers. However, to confirm that the precipitation factor produces realistic precipitation values, we adjusted the standard deviation of the simulated mass balance to the observed mass balance, a method similar to that proposed in Marzeion et al. (2012) and Mausson et al. (2019). Additional uncertainties in the calibrated melt factors come from the climate and geodetic mass balance datasets used to run and calibrate the model. Indeed, the melting temperature threshold establishes the onset of melting and influences the number of months in which it occurs. On the other hand, the geodetic mass balance defines the accumulated gain or loss per glacier over the calibration period, which in this case spans 20 years. Based on our evaluation of the corrected TerraClimate temperature and simulated mass balance, we correctly reproduce the seasonal melt distribution, associated with a mean underestimated overall annual mass balance of 185 mm w.e. yr<sup>-1</sup> which, however, is correlated with the in situ data ( $r = 0.7$ ). According to Rounce et al. (2020), similar results of glacier surface mass balance could be due to different combinations of model parameters. For instance, a wetter (or dryer) and warmer (or colder) parameter set – where high (or low) precipitation factors are compensated by high (or low) temperature biases – can lead to similar recent glacier mass changes and projections. Conversely, the implications for glacier runoff are likely to be significant for both recent and future simulations. In a wetter (or dryer) and warmer (or colder) scenario, there would be increased (or decreased) precipitation and melt, resulting in larger (or smaller) glacier runoff contribution. To address this, we obtained realistic values for precipitation and temperature based on in situ spatially distributed measurements and on our field experiences on monitored Andean glaciers. Furthermore, our evaluation of simulations in the three selected catchments enabled us to estimate glacier runoff amounts in the same order of magnitude as that of previous reports. However, caution must be exercised when using the calibrated melt factors estimated in the tropical Andes. This is because the temperature in this region was overestimated by an average of 2.4 °C, impacting the calibration of the melt factor values. These values should be lower than those estimated here (see Fig. 3).

With regard to the structural limitations of the model, it would be relevant to distinguish between ice and snowmelt when simulating the glacier melt with two melt factors. In addition, the sublimation on the glacier surface is very relevant in some glaciers located in the tropical Andes and Dry Andes 1 (Rabatel et al., 2011; MacDonell et al., 2013). However, the OGGM model does not incorporate these processes in glacier runoff and mass balance simulations.

## 5 Conclusion

In this study, we present a detailed quantification of the glacio-hydrological evolution across the Andes (11° N to 55° S) over the period 2000–2019 using OGGM. Our simulations rely on a glacier-by-glacier calibration of the changes in glacier volume. Simulations cover 11 282 km<sup>2</sup> of the glacierized surface area across the Andes, taking into account that calving glaciers (mostly in the Patagonian Icefields and Cordillera Darwin) were not considered because calving is not accounted for in the version of the glaciological model used here. The simulations were performed for the first time employing the same methodological approach, a corrected climate forcing, and parameter calibration at the glaciological zone scale throughout the Andes. Evaluation of our simulation outputs spanned glacier-specific and catchment scales, integrating in situ observations – which is uncommon in regional studies. From our results, we can conclude the following.

In relation to glacier runoff composed by glacier melt and rainfall on glaciers at the catchment scale, the largest percentage of studied Andean catchments encompassing 84 % of the total (661 catchments) presented an increase of 12 % in the mean annual glacier melt (ice melt and snowmelt) between the periods 2000–2009 and 2010–2019. These catchments present glaciers with higher elevation, larger size, and a lower mean annual temperature as well as a higher mean annual precipitation compared with glaciers located in catchments that showed a decrease in glacier melt in the same period which comprise just 12 % of studied catchments. Additionally, the mean annual rainfall on glaciers between the periods 2000–2009 and 2010–2019 exhibited a reduction of –2 %.

Special attention must be directed toward the tropical and Dry Andes regions, as they exhibited the most significant percentage increase in glacier runoff between the periods 2000–2009 and 2010–2019, reaching up to 40 % due to glacier melt and 3 % due to increased rainfall on glaciers over the past decade. Specifically, Dry Andes 1 exhibited a remarkable 62 % increase, while the inner tropic zone exhibited a 73 % rise in glacier runoff in the same periods. Notably, these particular glaciological zones displayed the smallest absolute quantities of glacier runoff across the entire Andes region. Dry Andes 1 emerges as the most vulnerable glaciological zone to glacier runoff water scarcity in the Andes.

Three catchments (La Paz, Maipo, and Baker) located in contrasting climatic and morphometric zones (glaciological zones) are used to evaluate the simulations. Our results show consistency with previous studies and in situ observations. The larger glacier runoff contributions to the catchment water flows during the period 2000–2019 are quantified for the Baker (43 %) and Maipo (36 %) catchments during the summer season (January to March). On the other hand, the larger glacier runoff contribution to the La Paz catchment (45 %) was estimated during the transition season (September to November).

The correction of temperature and precipitation data, coupled with parameter calibration conducted at the glaciological zone scale, enabled us to obtain annual estimates of glacier mass balance and runoff closer to what has been measured in glaciers and some Andean catchments, highlighting the estimation of annual temperature lapse rates and variability in glacier mass balance through measurements to correct climate data across distinct glaciological zones. This improvement not only ensures better alignment with local observations but also establishes a more robust tool for forecasting future glacier runoff patterns in the Andes. This method stands apart from global models by specifically addressing the local climate and parameter values inherent to the Andean region.

Lastly, our results help to improve knowledge about the hydrological responses of glacierized catchments across the Andes through the correction of inputs, calibration by glaciers, and validation of our simulations considering different glaciological zones. The implementation of this model during the historical period is a prerequisite for simulating the future evolution of the Andean glaciers.

*Code and data availability.* Data per glacier in this study are available at <https://doi.org/10.5281/zenodo.7890462> (Caro, 2023).

*Supplement.* The supplement related to this article is available online at: <https://doi.org/10.5194/tc-18-2487-2024-supplement>.

*Author contributions.* AC, TC, and AR were involved in the study design. AC wrote the model implementation and produced the figures, tables, and first draft of the manuscript. NC contributed to the model implementation. AC and NG carried out the data curation and TerraClimate temperature evaluation. AC performed the first level of analysis, which was improved by input from TC, AR, NC, and FS. All authors contributed to the review and editing of the paper.

*Competing interests.* The contact author has declared that none of the authors has any competing interests.

*Disclaimer.* Publisher's note: Copernicus Publications remains neutral with regard to jurisdictional claims made in the text, published maps, institutional affiliations, or any other geographical representation in this paper. While Copernicus Publications makes every effort to include appropriate place names, the final responsibility lies with the authors.

*Acknowledgements.* We acknowledge LabEx OSUG@2020 (Investissement d'Avenir, ANR10LABX56). Alexis Caro thanks Shelley MacDonell (University of Canterbury – CEAZA), Ashley Apey (Geoestudios), Marius Schaefer (U. Austral de Chile), and Claudio Bravo as well as Sebastián Cisternas (CECs, Centro de Estudios Científicos de Valdivia) for the data provided. In addition, Alexis Caro thanks the OGGM support team, especially Patrick Schmitt, Lilian Schuster, Larissa van der Laan, Anouk Vlug, Rodrigo Aguayo, and Fabien Maussion. Lastly, Alexis Caro greatly appreciates discussing the results for specific glaciers or catchments with Ezequiel Toum (IANIGLA, Argentina), Álvaro Ayala (CEAZA, Chile), Lucas Ruiz (IANIGLA, Argentina), Gabriella Collao (IGE, Univ. Grenoble Alpes, France), Diego Cusicanqui (IGE-ISTerre, Univ. Grenoble Alpes, France), and David Farías-Barahona (FAU, U. de Concepción, Chile).

All authors are grateful for the comments provided by the two anonymous reviewers and by the editor, which helped considerably improve the scientific quality of this article.

*Financial support.* This study was conducted as part of the International Joint Laboratory GREAT-ICE and the Service National d'Observation GLACIOCLIM (<https://glacioclim.osug.fr>, last access: July 2022), two joint initiatives of the IRD; universities/institutions in Bolivia, Peru, Ecuador, and Colombia; and the IRN-ANDES-C2H. This research was funded by the National Agency for Research and Development (ANID)/Scholarship Program/DOCTORADO BECAS CHILE/2019-72200174. This work was also supported by the CLIMAT AmSud project AndeSnow (grant no. CLI2020006).

*Review statement.* This paper was edited by Ben Marzeion and reviewed by two anonymous referees.

## References

- Abatzoglou, J. T., Dobrowski, S. Z., Parks, S. A., and Hegewisch, K. C.: TerraClimate, a High-Resolution Global Dataset of Monthly Climate and Climatic Water Balance from 1958–2015, *Sci. Data*, 5, 1–12, <https://doi.org/10.1038/sdata.2017.191>, 2018.
- Alvarez-Garreton, C., Mendoza, P. A., Boisier, J. P., Aador, N., Galleguillos, M., Zambrano-Bigiarini, M., Lara, A., Puelma, C., Cortes, G., Garreaud, R., McPhee, J., and Ayala, A.: The CAMELS-CL dataset: catchment attributes and meteorology for large sample studies – Chile dataset, *Hydrol. Earth Syst. Sci.*, 22, 5817–5846, <https://doi.org/10.5194/hess-22-5817-2018>, 2018.
- Autin, P., Sicart, J. E., Rabatel, A., Soruco, A., and Hock, R.: Climate Controls on the Interseasonal and Interannual Variability of the Surface Mass and Energy Balances of a Tropical Glacier (Zongo Glacier, Bolivia, 16° S): New Insights From the Multi-Year Application of a Distributed Energy Balance Model, *J. Geophys. Res.-Atmos.*, 127, e2021JD035410, <https://doi.org/10.1029/2021JD035410>, 2022.
- Ayala, Á., Pellicciotti, F., MacDonell, S., McPhee, J., and Bur-lando, P.: Patterns of glacier ablation across North-Central Chile: Identifying the limits of empirical melt models under sublimation-favorable conditions, *Water Resour. Res.*, 53, 5601–5625, <https://doi.org/10.1002/2016WR020126>, 2017.
- Ayala, Á., Farías-Barahona, D., Huss, M., Pellicciotti, F., McPhee, J., and Farinotti, D.: Glacier runoff variations since 1955 in the Maipo River basin, in the semiarid Andes of central Chile, *The Cryosphere*, 14, 2005–2027, <https://doi.org/10.5194/tc-14-2005-2020>, 2020.
- Baraer, M., Mark, B. G., Mckenzie, J. M., Condom, T., Bury, J., Huh, K.-I., Portocarrero, C., Gómez, J., and Rathay, S.: Glacier Recession and Water Resources in Peru's Cordillera Blanca, *J. Glaciol.*, 58, 134–150, <https://doi.org/10.3189/2012JoG11J186>, 2012.
- Basantes-Serrano, R., Rabatel, A., Francou, B., Vincent, C., Soruco, A., Condom, T., and Ruíz, J. C.: New insights into the decadal variability in glacier volume of a tropical ice cap, Antisana (0°29' S, 78°09' W), explained by the morpho-topographic and climatic context, *The Cryosphere*, 16, 4659–4677, <https://doi.org/10.5194/tc-16-4659-2022>, 2022.
- Braun, L. N. and Renner, C. B.: Application of a conceptual runoff model in different physiographic regions of Switzerland, *Hydrolog. Sci. J.*, 37, 217–231, 1992.
- Bravo, C., Loriaux, T., Rivera, A., and Brock, B. W.: Assessing glacier melt contribution to streamflow at Universidad Glacier, central Andes of Chile, *Hydrol. Earth Syst. Sci.*, 21, 3249–3266, <https://doi.org/10.5194/hess-21-3249-2017>, 2017.
- Burger, F., Ayala, A., Farias, D., Shaw, T. E., MacDonell, S., Brock, B., McPhee, J., and Pellicciotti, F.: Interannual Variability in Glacier Contribution to Runoff from a High-elevation Andean Catchment: Understanding the Role of Debris Cover in Glacier Hydrology, *Hydrol. Process.*, 33, 214–229, <https://doi.org/10.1002/hyp.13354>, 2019.
- Caro, A.: Estudios glaciológicos en los nevados de Chillán, University of Chile, Santiago, [thesis], <https://repositorio.uchile.cl/handle/2250/116536> (last access: September 2022), 2014.
- Caro, A.: Hydrological Response of Andean Catchments to Recent Glacier Mass Loss (data), Zenodo [data set], <https://doi.org/10.5281/zenodo.7890462>, 2023.
- Caro, A., Condom, T., and Rabatel, A.: Climatic and Morphometric Explanatory Variables of Glacier Changes in the Andes (8–55° S): New Insights From Machine Learning Approaches, *Front. Earth Sci.*, 9, 713011, <https://doi.org/10.3389/feart.2021.713011>, 2021.
- Cauvy-Fraunié, S. and Dangles, O.: A Global Synthesis of Biodiversity Responses to Glacier Retreat. *Nat. Ecol. Evol.* 3 (12), 1675–1685, <https://doi.org/10.1038/s41559-019-1042-8>, 2019.
- CEAZA: Datos meteorológicos de Chile, Centro de Estudios Avanzados en Zonas Áridas [data set], <http://www.ceazamet.cl/> (last access: July 2022), 2022.
- CECs: Meteorological data measured by Centro de Estudios Científicos, Centro de Estudios Científicos, 2018.
- Condom, T., Escobar, M., Purkey, D., Pouget, J. C., Suarez, W., Ramos, C., Apaestegui, J., Zapata, M., Gomez, J., and Vergara,

- W.: Modelling the hydrologic role of glaciers within a Water Evaluation and Planning System (WEAP): a case study in the Rio Santa watershed (Peru), *Hydrol. Earth Syst. Sci. Discuss.*, 8, 869–916, <https://doi.org/10.5194/hessd-8-869-2011>, 2011.
- Crippen, R., Buckley, S., Agram, P., Belz, E., Gurrola, E., Hensley, S., Kobrick, M., Lavalle, M., Martin, J., Neumann, M., Nguyen, Q., Rosen, P., Shimada, J., Simard, M., and Tung, W.: NASA-DEM Global Elevation Model: Methods and Progress. *The International Archives of the Photogrammetry, Remote Sensing and Spatial Information Sciences*, XLI-B4, 125–128. (20), 2016.
- Devenish, C. and Gianella, C.: Sustainable Mountain Development in the Andes. 20 Years of Sustainable Mountain Development in the Andes – from Rio 1992 to 2012 and beyond, CONDESAN, Lima, Peru, 2012.
- DGA: Datos de estudios hidroglaciológicos de Chile, Dirección General de Aguas [data set], <https://snia.mop.gob.cl> (last access: July 2022), 2022.
- Dussaillant, A., Buytaert, W., Meier, C., and Espinoza, F.: Hydrological regime of remote catchments with extreme gradients under accelerated change: the Baker basin in Patagonia, *Hydrolog. Sci. J.*, 57, 1530–1542, <https://doi.org/10.1080/02626667.2012.726993>, 2012.
- Dussaillant, I., Berthier, E., Brun, F., Masiokas, M., Hugonnet, R., Favier, V., Rabatel, A., Pitte, P., and Ruiz, L.: Two Decades of Glacier Mass Loss along the Andes, *Nat. Geosci.*, 12, 802–808, <https://doi.org/10.1038/s41561-019-0432-5>, 2019.
- Fariás-Barahona, D., Wilson, R., Bravo, C., Vivero, S., Caro, A., Shaw, T. E., Casassa, G., Ayala, A., Mejías, A., Harrison, S., Glasser, N. F., McPhee, J., Wünderlich, O., and Braun, M.: A Near 90-year Record of the Evolution of El Morado Glacier and its Proglacial lake, Central Chilean Andes, *J. Glaciol.*, 66, 846–860, <https://doi.org/10.1017/jog.2020.52>, 2020.
- Farinotti, D., Huss, M., Bauder, A., Funk, M., and Truffer, M.: A method to estimate the ice volume and ice-thickness distribution of alpine glaciers, *J. Glaciol.*, 55, 422–430, <https://doi.org/10.3189/002214309788816759>, 2009.
- Farinotti, D., Huss, M., Fürst, J. J., Landmann, J., Machguth, H., Maussion, F., and Pandit, A.: A consensus estimate for the ice thickness distribution of all glaciers on Earth, *Nat. Geosci.*, 12, 168–173, <https://doi.org/10.1038/s41561-019-0300-3>, 2019.
- Favier, V., Wagnon, P., Chazarin, J.-P., Maisincho, L., and Coudrain, A.: One-year measurements of surface heat budget on the ablation zone of Antizana glacier 15, Ecuadorian Andes, *J. Geophys. Res.*, 109, D18105, <https://doi.org/10.1029/2003JD004359>, 2004.
- Fukami, H. and Naruse, R.: Ablation of ice and heat balance on Soler glacier, Patagonia, *Bulletin of Glacier Research*, 4, 37–42, 1987.
- Gao, L., Bernhardt, M., and Schulz, K.: Elevation correction of ERA-Interim temperature data in complex terrain, *Hydrol. Earth Syst. Sci.*, 16, 4661–4673, <https://doi.org/10.5194/hess-16-4661-2012>, 2012.
- Garreaud, R. D., Alvarez-Garretón, C., Barichivich, J., Boisier, J. P., Christie, D., Galleguillos, M., LeQuesne, C., McPhee, J., and Zambrano-Bigiarini, M.: The 2010–2015 megadrought in central Chile: impacts on regional hydroclimate and vegetation, *Hydrol. Earth Syst. Sci.*, 21, 6307–6327, <https://doi.org/10.5194/hess-21-6307-2017>, 2017.
- Gascoïn, S., Kinnard, C., Ponce, R., Lhermitte, S., MacDonell, S., and Rabatel, A.: Glacier contribution to streamflow in two headwaters of the Huasco River, Dry Andes of Chile, *The Cryosphere*, 5, 1099–1113, <https://doi.org/10.5194/tc-5-1099-2011>, 2011.
- GLACIOCLIM: Données météorologiques, Service d’Observation GLACIOCLIM [data set], <https://glacioclim.osug.fr/Donnees-des-Andes> (last access: July 2022), 2022.
- Guido, Z., McIntosh, J. C., Papuga, S. A., and Meixner, T.: Seasonal Glacial Meltwater Contributions to Surface Water in the Bolivian Andes: A Case Study Using Environmental Tracers, *J. Hydrol. Reg. Stud.*, 8, 260–273, <https://doi.org/10.1016/j.ejrh.2016.10.002>, 2016.
- Hernández, J., Mazzorana, B., Loriaux, T., and Iribarren, P.: Reconstrucción de caudales en la Cuenca Alta del Río Huasco, utilizando el modelo Cold Regional Hydrological Model (CRHM), AAGG2021, 2021.
- Hock, R.: Temperature index melt modelling in mountain areas, *J. Hydrol.*, 282, 104–115, [https://doi.org/10.1016/S0022-1694\(03\)00257-9](https://doi.org/10.1016/S0022-1694(03)00257-9), 2003.
- Hugonnet, R., McNabb, R., Berthier, E., Menounos, B., Nuth, C., Girod, L., Farinotti, D., Huss, M., Dussaillant, I., Brun, F., and Kääh, A.: Accelerated global glacier mass loss in the early twenty-first century, *Nature*, 592, 726–731, <https://doi.org/10.1038/s41586-021-03436-z>, 2021.
- Huss, M. and Hock, R.: A new model for global glacier change and sea-level rise, *Front. Earth Sci.*, 3, 54, <https://doi.org/10.3389/feart.2015.00054>, 2015.
- Huss, M. and Hock, R.: Global-scale hydrological response to future glacier mass loss, *Nat. Clim. Change*, 8, 135–140, <https://doi.org/10.1038/s41558-017-0049-x>, 2018.
- IANIGLA: Datos meteorológicos, Instituto Argentino de Nivología, Glaciología y Ciencias Ambientales [data set], <https://observatorioandino.com/estaciones/> (last access: July 2022), 2022.
- Kienholz, C., Rich, J. L., Arendt, A. A., and Hock, R.: A new method for deriving glacier centerlines applied to glaciers in Alaska and northwest Canada, *The Cryosphere*, 8, 503–519, <https://doi.org/10.5194/tc-8-503-2014>, 2014.
- Koizumi, K. and Naruse, R.: Measurements of meteorological conditions and ablation at Tyndall Glacier, Southern Patagonia, in December 1990, *Bulletin of Glacier Research*, 10, 79–82, 1992.
- Krogh, S. A., Pomeroy, J. W., and McPhee, J.: Physically based hydrological modelling using reanalysis data in Patagonia, *J. Hydrometeorol.*, 16, 172–193, <https://doi.org/10.1175/JHM-D-13-0178.1>, 2014.
- Lehner, B. and Grill, G.: Global river hydrography and network routing: baseline data and new approaches to study the world’s large river systems, *Hydrol. Process.*, 27, 2171–2186, <https://doi.org/10.1002/hyp.9740>, 2013.
- MacDonell, S., Kinnard, C., Mölg, T., Nicholson, L., and Abermann, J.: Meteorological drivers of ablation processes on a cold glacier in the semi-arid Andes of Chile, *The Cryosphere*, 7, 1513–1526, <https://doi.org/10.5194/tc-7-1513-2013>, 2013.
- Malmros, J. K., Mernild, S. H., Wilson, R., Yde, J. C., and Fensholt, R.: Glacier Area Changes in the central Chilean and Argentinean Andes 1955–2013/14, *J. Glaciol.*, 62, 391–401, <https://doi.org/10.1017/jog.2016.43>, 2016.
- Marangunic, C., Ugalde, F., Apey, A., Armendáriz, I., Bustamante, M., and Peralta, C.: Ecosistemas de montaña de la cuenca alta del

- río Mapocho, Glaciares en la cuenca alta del río Mapocho: variaciones y características principales, AngloAmerican – CAPES UC, Santiago de Chile, 2021.
- Mark, B. and Seltzer, G.: Tropical glacier meltwater contribution to stream discharge: A case study in the Cordillera Blanca, Peru, *J. Glaciol.*, 49, 271–281, <https://doi.org/10.3189/172756503781830746>, 2003.
- Marzeion, B., Jarosch, A. H., and Hofer, M.: Past and future sea-level change from the surface mass balance of glaciers, *The Cryosphere*, 6, 1295–1322, <https://doi.org/10.5194/tc-6-1295-2012>, 2012.
- Masiokas, M. H., Christie, D. A., Le Quesne, C., Pitte, P., Ruiz, L., Villalba, R., Luckman, B. H., Berthier, E., Nussbaumer, S. U., González-Reyes, Á., McPhee, J., and Barcaza, G.: Reconstructing the annual mass balance of the Echaurren Norte glacier (Central Andes, 33.5° S) using local and regional hydroclimatic data, *The Cryosphere*, 10, 927–940, <https://doi.org/10.5194/tc-10-927-2016>, 2016.
- Masiokas, M. H., Rabatel, A., Rivera, A., Ruiz, L., Pitte, P., Ceballos, J. L., Barcaza, G., Soruco, A., Bown, F., Berthier, E., Dussaillant, I., and MacDonell, S.: A Review of the Current State and Recent Changes of the Andean Cryosphere, *Front. Earth Sci.*, 8, 1–27, <https://doi.org/10.3389/feart.2020.00099>, 2020.
- Mateo, E. I., Mark, B. G., Hellström, R. Å., Baraer, M., McKenzie, J. M., Condom, T., Rapre, A. C., Gonzales, G., Gómez, J. Q., and Encarnación, R. C. C.: High-temporal-resolution hydrometeorological data collected in the tropical Cordillera Blanca, Peru (2004–2020), *Earth Syst. Sci. Data*, 14, 2865–2882, <https://doi.org/10.5194/essd-14-2865-2022>, 2022.
- Maussion, F., Butenko, A., Champollion, N., Dusch, M., Eis, J., Fourteau, K., Gregor, P., Jarosch, A. H., Landmann, J., Oesterle, F., Recinos, B., Rothenpieler, T., Vlug, A., Wild, C. T., and Marzeion, B.: The Open Global Glacier Model (OGGM) v1.1, *Geosci. Model Dev.*, 12, 909–931, <https://doi.org/10.5194/gmd-12-909-2019>, 2019.
- Meier, W. J.-H., Griebinger, J., Hochreuther, P., and Braun, M. H.: An Updated Multi-Temporal Glacier Inventory for the Patagonian Andes With Changes Between the Little Ice Age and 2016, *Front. Earth Sci.*, 6, 62, <https://doi.org/10.3389/feart.2018.00062>, 2018.
- Millan, R., Mougnot, J., Rabatel, A., and Morlighem, M.: Ice velocity and thickness of the world's glaciers, *Nat. Geosci.*, 15, 124–129, <https://doi.org/10.1038/s41561-021-00885-z>, 2022.
- NASA JPL: NASADEM Merged DEM Global 1 arc second V001 [Data set], NASA EOSDIS Land Processes DAAC, [https://doi.org/10.5067/MEaSURES/NASADEM/NASADEM\\_HGT.001](https://doi.org/10.5067/MEaSURES/NASADEM/NASADEM_HGT.001), 2020.
- Rabassa, J.: El cambio climático global en la Patagonia desde el viaje de Charles Darwin hasta nuestros días, *Revista de la Asociación Geológica Argentina*, 67, 139–156, 2010.
- Rabatel, A., Castebrunet, H., Favier, V., Nicholson, L., and Kinnard, C.: Glacier changes in the Pascua-Lama region, Chilean Andes (29° S): recent mass balance and 50 yr surface area variations, *The Cryosphere*, 5, 1029–1041, <https://doi.org/10.5194/tc-5-1029-2011>, 2011.
- Rabatel, A., Bermejo, A., Loarte, E., Soruco, A., Gomez, J., Leonardini, G., Vincent, C., and Sicart, J. E.: Relationship between snowline altitude, equilibrium-line altitude and mass balance on outer tropical glaciers: Glaciar Zongo – Bolivia, 16° S and Glaciar Artesonraju – Peru, 9° S, *J. Glaciol.*, 58, 1027–1036, <https://doi.org/10.3189/2012JoG12J027>, 2012.
- Rabatel, A., Francou, B., Soruco, A., Gomez, J., Cáceres, B., Ceballos, J. L., Basantes, R., Vuille, M., Sicart, J.-E., Huggel, C., Scheel, M., Lejeune, Y., Arnaud, Y., Collet, M., Condom, T., Consoli, G., Favier, V., Jomelli, V., Galarraga, R., Ginot, P., Maisincho, L., Mendoza, J., Ménégoz, M., Ramirez, E., Ribstein, P., Suarez, W., Villacis, M., and Wagnon, P.: Current state of glaciers in the tropical Andes: a multi-century perspective on glacier evolution and climate change, *The Cryosphere*, 7, 81–102, <https://doi.org/10.5194/tc-7-81-2013>, 2013.
- Ragettli, S. and Pellicciotti, F.: Calibration of a Physically Based, Spatially Distributed Hydrological Model in a Glaciated basin: On the Use of Knowledge from Glaciometeorological Processes to Constrain Model Parameters, *Water Resour. Res.*, 48, 1–20, <https://doi.org/10.1029/2011WR010559>, 2012.
- RGI Consortium: Randolph Glacier Inventory – A Dataset of Global Glacier Outlines, Version 6, NSIDC: National Snow and Ice Data Center, Boulder, Colorado, USA, <https://doi.org/10.7265/4m1f-gd79>, 2017.
- Rivera, A.: Mass balance investigations at Glaciar Chico, Southern Patagonia Icefield, Chile, PhD thesis, University of Bristol, Bristol, UK, 303 pp, 2004.
- Robson, B. A., MacDonell, S., Ayala, Á., Bolch, T., Nielsen, P. R., and Vivero, S.: Glacier and rock glacier changes since the 1950s in the La Laguna catchment, Chile, *The Cryosphere*, 16, 647–665, <https://doi.org/10.5194/tc-16-647-2022>, 2022.
- Rounce, D. R., Khurana, T., Short, M. B., Hock, R., Shean, D. E., and Brinkerhoff, D. J.: Quantifying parameter uncertainty in a large-scale glacier evolution model using Bayesian inference: application to High Mountain Asia, *J. Glaciol.*, 66, 175–187, <https://doi.org/10.1017/jog.2019.91>, 2020.
- Ruiz, L., Berthier, E., Viale, M., Pitte, P., and Masiokas, M. H.: Recent geodetic mass balance of Monte Tronador glaciers, northern Patagonian Andes, *The Cryosphere*, 11, 619–634, <https://doi.org/10.5194/tc-11-619-2017>, 2017.
- Schaefer, M., Rodriguez, J., Scheiter, M., and Casassa, G.: Climate and surface mass balance of Mocho Glacier, Chilean Lake District, 40° S, *J. Glaciol.*, 63, 218–228, <https://doi.org/10.1017/jog.2016.129>, 2017.
- Schuster, L., Rounce, D. R., and Maussion, F.: Glacier projections sensitivity to temperature-index model choices and calibration strategies, *Ann. Glaciol.*, 1–16, <https://doi.org/10.1017/aog.2023.57>, 2023.
- Seehaus, T., Malz, P., Sommer, C., Lippl, S., Cochachin, A., and Braun, M.: Changes of the tropical glaciers throughout Peru between 2000 and 2016 – mass balance and area fluctuations, *The Cryosphere*, 13, 2537–2556, <https://doi.org/10.5194/tc-13-2537-2019>, 2019.
- Seehaus, T., Malz, P., Sommer, C., Soruco, A., Rabatel, A., and Braun, M.: Mass balance and area changes of glaciers in the Cordillera Real and Tres Cruces, Bolivia, between 2000 and 2016, *J. Glaciol.*, 66, 124–136, <https://doi.org/10.1017/jog.2019.94>, 2020.
- SENAMHI: Datos hidrometeorológicos de Perú, Servicio Nacional de Meteorología e Hidrología del Perú [data set], <https://www.senamhi.gob.pe/?&=descarga-datos-hidrometeorologicos> (last access: July 2022), 2022.

- Shaw, T. E., Caro, A., Mendoza, P., Ayala, Á., Pellicciotti, F., Gascoin, S., and McPhee, J.: The Utility of Optical Satellite Winter Snow Depths for Initializing a Glacio-Hydrological Model of a High-Elevation, Andean Catchment, *Water Resour. Res.*, 56, 1–19, <https://doi.org/10.1029/2020WR027188>, 2020.
- Sicart, J. E., Wagnon, P., and Ribstein, P.: Atmospheric controls of heat balance of Zongo Glacier (16° S, Bolivia), *J. Geophys. Res.*, 110, D12106, <https://doi.org/10.1029/2004JD005732>, 2005.
- Sicart, J. E., Ribstein, P., Francou, B., Pouyaud, B., and Condom, T.: Glacier mass balance of tropical Zongo Glacier, Bolivia, comparing hydrological and glaciological methods, *Global Planet. Change*, 59, 27–36, <https://doi.org/10.1016/j.gloplacha.2006.11.024>, 2007.
- Sicart, J. E., R. Hock, and Six, D.: Glacier melt, air temperature, and energy balance in different climates: The Bolivian Tropics, the French Alps, and northern Sweden, *J. Geophys. Res.*, 113, D24113, <https://doi.org/10.1029/2008JD010406>, 2008.
- Soruco, A., Vincent, C., Rabatel, A., Francou, B., Thibert, E., Sicart, J. E., and Condom, T.: Contribution of Glacier Runoff to Water Resources of La Paz City, Bolivia (16° S), *Ann. Glaciol.*, 56, 147–154, <https://doi.org/10.3189/2015AoG70A001>, 2015.
- Stuefer, M.: Investigations on Mass Balance and Dynamics of Moreno Glacier Based on Field Measurements and Satellite Imagery, Ph.D. Dissertation, University of Innsbruck, Innsbruck, 1999.
- Takeuchi, Y., Naruse, R., and Satow, K.: Characteristics of heat balance and ablation on Moreno and Tyndall glaciers, Patagonia, in the summer 1993/94, *Bulletin of Glacier Research*, 13, 45–56, 1995.
- WGMS: Global Glacier Change Bulletin No. 4 (2018–2019), edited by: Zemp, M., Nussbaumer, S. U., Gärtner-Roer, I., Bannwart, J., Paul, F., and Hoelzle, M., ISC (WDS)/IUGG (IACS)/UNEP/UNESCO/WMO, World Glacier Monitoring Service, Zurich, Switzerland, 278 pp., Based on database version, <https://doi.org/10.5904/wgms-fog-2021-05>, 2021.
- Zhang, G. Q., Bolch, T., Yao, T. D., Rounce, D. R., Chen, W. F., Veh, G., King, O., Allen, S. K., Wang, M. M., and Wang, W. C.: Underestimated mass loss from lake-terminating glaciers in the greater Himalaya, *Nat. Geosci.*, 16, 333–338, <https://doi.org/10.1038/s41561-023-01150-1>, 2023.
- Zimmer, A., Meneses, R. I., Rabatel, A., Soruco, A., Dangles, O., and Anthelme, F.: Time Lag between Glacial Retreat and Upward Migration Alters Tropical alpine Communities, *Perspect. Plant Ecol.*, 30, 89–102, <https://doi.org/10.1016/j.ppees.2017.05.003>, 2018.